Université de Lorraine
Lappeenranta University of Technology
Luleå Tekniska Universitet

José Perdomo

UE PERFORMANCE IN A 5G MULTI-CONNECTIVITY UDN CITY SCENARIO

Examiners: Prof. Eric Rondeau
Prof. Jari Porras
Prof. Karl Andersson

Supervisors: Mårten Ericson (Ericsson Research)
Mats Nordberg (Ericsson Research)
Karl Andersson (Luleå Tekniska Universitet)

This thesis is prepared as part of an European Erasmus Mundus programme PERCCOM - PERvasive Computing & COMmunications for sustainable development [1].

This thesis has been accepted by partner institutions of the consortium (cf. UDL-DAJ, n°1524, 2012 PERCCOM agreement). Successful defense of this thesis is obligatory for graduation with the following national diplomas:

- Master in Complex Systems Engineering (University of Lorraine)
- Master of Science in Technology (Lappeenranta University of Technology)
- Master in Pervasive Computing and Communications for Sustainable Development (Luleå Tekniska Universitet)

ABSTRACT

Université de Lorraine
Lappeenranta University of Technology
Luleå Tekniska Universitet

José Perdomo

UE Performance in a 5G Multi-connectivity UDN City Scenario

Master's Thesis Dissertation

84 pages, 33 figures, 12 tables, 1 appendix

Examiners: Prof. Eric Rondeau
Prof. Jari Porras
Prof. Karl Andersson

Keywords: Multi-connectivity, UE, ultra-dense networks, urban city scenario, mmWave.

Multi-connectivity and network densification are two solutions intended to enhance user throughput and reliability. These solutions are critical since 5G NR uses a wide range of frequency bands, which exhibit different varying radio coverage characteristics. This work studies the user equipment (UE) performance using multi-connectivity within an ultra-dense network (UDN) deployed in an urban city environment.

By being connected to more than one access node simultaneously, the UE should benefit from increased reliability and data rates at the expense of a potentially increased power consumption. In this letter, we have constructed an urban city environment and a context-aware UE power consumption model. The performance of the UE is assessed with an uplink power control scheme for multi-connectivity and a novel multi-connectivity scheme is proposed.

Our simulation results show that dual-connectivity increases performance by up to 44% and 27% in average downlink and uplink throughput, respectively. Similarly, tri-connectivity

does the same by up to 45% and 25%. At mid load (forty-five users), the average increase in UE power consumption compared to single-connectivity is 25% and 60% for dual-connectivity and tri-connectivity, respectively. Dual-connectivity increases global UE energy efficiency by up to 30%. Within an urban environment, dual-connectivity decreases the RLF rate by 20% compared to single-connectivity for high speed users.

ACKNOWLEDGEMENTS

Luleå, June 06, 2019

I would like to give an immense thank you to the PERCCOM consortium which provided me the opportunity to take part in this master's degree two years ago. During this period, I have grown at a personal, professional and academic level, and that's thanks to the great master's programme Eric, Jari, Karl, JPG and others have built.

Special thanks to my supervisors Karl, Mats and Mårten. I would like to thank Karl for always providing me assistance and motivation to push forward; Mats, for the support and the sport activities; and Mårten, for the mentorship during this period at Ericsson.

I would also like to give special thanks to my cohort-mates: Amir, An, Anastasiia, Anisul, Askar, Daniel, Darren, Feruz, Florian, Ijlal, Krishna, Maliha, Mansour, Meru, Orsola, Sami, Sunnat, Valeria. Gracias a todos!

Sincerely,
José Perdomo

June 2019
Luleå, Sweden

TABLE OF CONTENTS

LIST OF FIGURES

LIST OF SYMBOLS AND ABBREVIATIONS

Abbreviations

5G	Fifth-generation of Mobile Communication
NR	New Radio
IoT	Internet of Things
WCDMA	Wideband Code Division Multiple Access
LTE	Long Term Evolution
UDN	Ultra-dense Networks
METIS-I	Mobile and wireless communications Enablers for Twenty-twenty (2020) Information Society
ITU-R	International Telecommunications Union - Radiocommunication Sector
IMT-2020	International Mobile Telecommunications - 2020 standard
3GPP	Third Generation Partnership Project
DC	Dual-connectivity
MC	Multi-connectivity
UE	User Equipment
RAT	Radio Access Technology
MIMO	Multiple-input multiple-output
eMBB	Enhanced Mobile Broadband
URLLC	Ultra-Reliable Low Latency Communications
mMTC	massive Machine-Type Communication
DL	Downlink
UL	Uplink
OFDM	Orthogonal Frequency Division Multiplex
5GCN	5G Core Network
RAN	Radio Access Network
CN	Core Network
eNB	evolved Node B
ng-eNB	Next Generation evolved Node B, abbreviated gNB
RRM	Radio Resource Management
UPF	User Plane Function
AMF	Access and Mobility Function

Xn	Interface that interconnects two gNB nodes
NSA	Non-standalone
NG-c	control plane interface between gNB and AMF
NG-u	control plane interface between gNB and UPF
EPC	Evolved Packet Core
mmWave	milimeter-Wave
FR2	Frequency Range 2, i.e. mmWave Band
FR1	Frequency Range 1, i.e. legacy Low Frequency Bands
CA	Carrier Aggregation
LTE-A	Long Term Evolution - Advanced
CoMP	Coordinated Multipoint
AS	Active Set of serving cells
SC	Single-connectivity
RLF	Radio-link Failure
QoE	Quality of Experience
CIO	Corrective Indicator Offset
MRO	Mobility Robustness Optimization
AaSE	Agnostic Air Slice Enabler
PDCP	Packet Data Convergence Protocol
LoS	Line of Sight
nLoS	non Line of Sight
PL	Path Loss
RF	Radio-Frequency
OS	Operating System
CSI-RS	Channel State Information - Reference Signals
SS	Synchronization Signal
SRS	Sounding Reference Signals
CQI	Channel Quality Indicator
RSRP	Referenced Signal Received Power
SINR	Signal-to-interference-plus-noise ratio
PHR	Power Headroom Report
RRC	Radio Resource Control
PUSCH	Physical Uplink Shared Channel
DRX	Discontinuous Reception
PDCCH	Physical Downlink Control Channel

MEC	Mobile Edge Computing
PA	Power Amplifier
RBS	Radio Base Station
HSPA	High Speed Packet Access
UMi	Urban Micro
UMa	Urban Macro
CDF	Cumulative Distributive Function
DUT	Device-under-test

1 INTRODUCTION

Traffic in mobile networks continues to increase exponentially [2]. New technologies such as virtual reality and augmented reality , among others, are becoming more widely adopted , and they are requiring even more data-intensive content [7]. By 2024, data traffic per active smartphone is expected to reach 39 GB in North America, as seen in Figure 1.1. Current forecasts estimate that the global mobile data traffic will reach 131 exabytes per month by the end of 2024 [2].

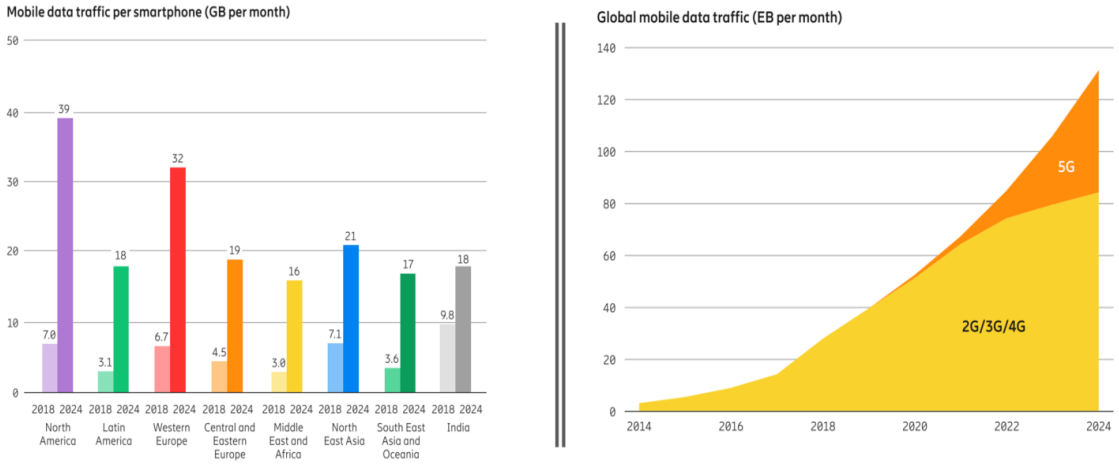

Figure 1.1: Smartphone Monthly Data Demand and Exponential Traffic Growth taken from [2]

Moreover, the increasing number of connected devices as a result of the Internet of Things (IoT), particularly those connected to the mobile network, i.e. cellular IoT, will probably pose challenges to the mobile network due to the predicted extremely high density of devices per cell. It is expected that the number of cellular IoT connections will reach 3.5 billion in 2023 [8]. Furthermore, technological innovations in other fields, such as the automotive and manufacturing industries, are requiring services from the mobile network. These novel uses cases pose new stringent requirements for the mobile network.

The telecommunications' industry and various institutions are aware of these challenges. In 2012, the system concept for the Fifth-generation of Mobile Communication (5G) was defined by METIS-I, the European Union's Flagship 5G Research Project, acronym for "Mobile and wireless communications Enablers for Twenty-twenty (2020) Information

Society". METIS derived so-called horizontal topics to build the overall system concept for 5G prior to standardization. Each horizontal topic addresses one or more uses cases developed within the project, with the intention to meet the specific requirements utilizing a subset of technology enablers. METIS-I identified Ultra-dense networks (UDNs), a solution based under the premise of improving the user's throughput and reliability via infrastructure densification [9], as an horizontal topic to address high traffic demands and be able to support reliable services.

In 2015, the International Telecommunications Union - Radiocommunication Sector (ITU-R) issued the minimum technical requirements for the 5G networks via the International Mobile Telecommunications - 2020 standard (IMT-2020). With the IMT framework in place, the responsibility to define the actual technical specification fell on the Third Generation Partnership Project (3GPP). 3GPP via its Release 15 specification established 5G New Radio (NR), 5G's new radio air interface.

A difference compared to previous mobile systems 3GPP has specified, such as Wideband Code Division Multiple Access (WCDMA) and Long Term Evolution (LTE), is that 5G is designed to be able to operate on a broad range of frequencies, from frequencies used today up to the mmWave band (i.e. frequencies around 30 GHz). Wireless communication at such frequency bands pose radio coverage challenges on urban environments due to its high path loss, high indoor penetration and low diffraction. Hence, the Release 15 specification defined LTE/NR dual-connectivity (DC) to leverage the already existing LTE infrastructure deployed on lower frequency bands to improve coverage. The interworking between LTE and NR has been defined as non-standalone 5G (NSA 5G). DC is the basis for this scenario. 5G NSA allows for early commercial deployments while 5G NR continues to evolve beyond Release 15.

In this regard, due to the stringent performance requirements defined for 5G, multi-connectivity (MC), the general case for DC, plays an important role. MC, enabled by network densification, allows the user equipment (UE) to be connected to multiple secondary base stations from different radio access technologies (RATs) to further increase performance and reliability, and ultimately meet the requirements for the envisioned 5G use cases.

1.1 Problem

The increasing average data demand per active user equipment has been one of the main contributors for the exponential traffic growth on mobile networks [7]. With each new generation of radio access technology (e.g. WCDMA and LTE) specified by 3GPP, the user data rates have been increased and NR is no exception. 3GPP has defined solutions via the NR specification such as: usage of mmWave frequencies, massive multiple-input multiple-output (MIMO), DC, and multiple numerologies, among others [4]. All of these new solutions may increase power consumption on the cellular subsystem of the next generation user equipment.

In addition, battery life has been one of the smartphone's components that hasn't had much improvement. In 10 years, wireless capacity for mobile terminals has increased by 10,000 times according to [10], while only 4-5 folds increment of battery specific power has been achieved [11]. Acceptable battery lifetime is necessary for the next generation user equipment. Mitigating UE power consumption will be critical towards the 5G evolution.

Furthermore, it is forecasted that by 2024, the amount of mobile subscriptions will reach 8.8 billion, where 1.9 billion will be 5G subscriptions, and nearly 5 billion will be LTE [8]. From a sustainability point of view, a modern mobile device as such consumes 7 kWh per year [10]. Although this figure individually may seem reasonable, the energy consumption aggregated across all the mobile subscriptions worldwide demands special attention. Recent 3GPP energy efficiency standards establish that energy savings should continue to be implemented at network, site and equipment level in a coordinated manner [12].

As described previously, multi-connectivity within an ultra-dense network allows the UE to be connected to a set of access nodes from multiple options from its vicinity. This scenario may increase UE power consumption due to the simultaneous transmission/reception in uplink and downlink across multiple carriers from different RATs. One of the main contributors for UE power consumption is the uplink transmit power [13], which in turn is highly dependent on the radio conditions.

1.2 AIM, RESEARCH OBJECTIVES AND QUESTIONS

The objective of this master thesis is to investigate the performance of the UE when using MC within an UDN deployed in an urban city environment. To achieve this objective, UE performance will be analyzed using a discrete system-level simulator. In order to appropriately model an urban city scenario, a comprehensive propagation model for low (2 GHz) and mmWave frequencies (26-28 GHz) for urban environments was integrated to the simulator for this study.

Simulations will be realized to study UE performance in terms of uplink and downlink throughput, power consumption, energy efficiency and reliability. Thereafter, a multi-connectivity scheme will be designed in order to improve the UE performance in terms of power consumption.

Research Questions

I. How does the use of multi-connectivity in an urban city scenario impact UE performance?

A) How does multi-connectivity improve uplink and downlink throughput in an urban city scenario?

B) What is the effect on the UE's power consumption using multi-connectivity?

C) To what extent does multi-connectivity improve reliability in a dense urban city scenario?

II. How does multi-connectivity schemes, designed for a specific purpose, improve UE performance in terms of power consumption in an ultra-dense network?

1.3 Delimitations

This master thesis focuses on analyzing the performance of the user equipment when using multi-connectivity in a dense urban city scenario. Performance is studied exclusively from the user equipment's perspective, more specifically the LTE and 5G NR cellular subsystem of the user equipment. This study emphasizes on the uplink but it also encompasses the downlink.

This work is done using system-level simulations. The study scenario takes place within an ultra-dense network deployed in a city. Following specific guidelines, we chose models for the network layout such that they resemble a metropolitan area with multi-story buildings and streets. Moreover, in order to capture the propagation characteristics for the mmWave band and midband, different models are used for each band with corresponding scattering objects that would be typical for a city scenario. We focus on Layer 2 and higher, i.e. we don't model Layer 1 components, such as fast fading, massive MIMO, beam forming, etc. Since this work was done using Ericsson's proprietary simulator, some details will be excluded.

1.4 Thesis Structure

This section provides an explanation of the structure of the report. Section 2 provides an overview of the technical details of the 5G NR specification that concern this study and related work concerning our study scenario. The latter also provides an overview of related work to save energy on the user equipment and also on mobility management schemes tailored for the user equipment. Section 4 illustrates useful concepts for our study scenario, and it provides a description of the metrics we used to assess UE performance. Section 5 describes the different systems models that comprise this study. Section 6 provides the results attained in our work and presents an evaluation of them. Section 7 presents the outcomes of our work, main findings and conclusions. This section provides the sustainability impact of our study and it also describes future paths to study the UE using MC.

2 BACKGROUND AND RELATED WORK

This chapter provides an overview of 5G. This chapter also describes a plethora of related work for our study scenario. Section 2.1 provides an overview of the 5G NR specification. Section 2.2 describes LTE/NR dual-connectivity and Section 2.3 describes its general case, multi-connectivity. Section 2.4 defines ultra-dense networks and Section 2.5 describes related work to model mmWave signal propagation in urban environments. Section 2.6 provides details about the user equipment in terms of power consumption and it also describes the procedures to communicate with the mobile network, e.g. uplink power control.

2.1 5G NR

5G is considered both a new radio access technology and also an umbrella term for a wide new range of novel applications and services. 5G NR and its evolution is expected to meet the minimum technical requirements defined in IMT-2020 in order to enable the envisioned usage scenarios. As shown in Figure 2.1, the requirements are meant to enable the following main usage scenarios: enhanced Mobile Broadband (eMBB), Ultra-Reliable Low Latency Communication (URLLC), massive Machine-Type Communication (mMTC) described in [14].

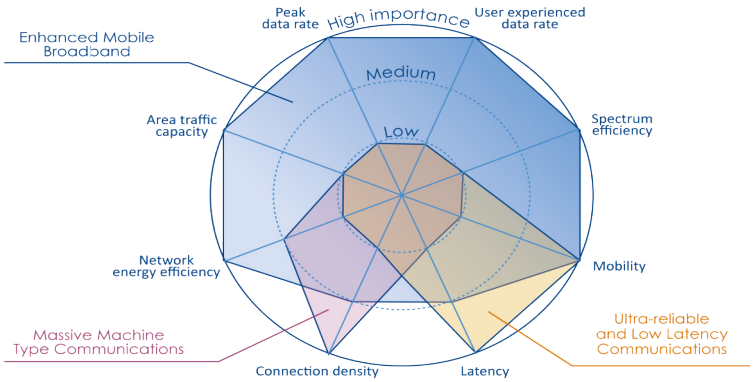

Figure 2.1: Minimum Technical Requirements defined in IMT-2020 mapped to its corresponding usage scenario

These requirements target 20 and 10 Gb/s peak data rates for downlink (DL) and uplink (UL) respectively [15]. In order to achieve such data rates, 3GPP has defined multiple solutions via the NR specification [4]. 5G NSA is intended to meet the requirements for the eMBB usage scenario.

Historically, there has been an asymmetry between downlink and uplink traffic. Due to the nature of most use cases, downlink traffic has been more than its uplink counterpart. Operators have dimensioned their networks according to downlink traffic since it requires more capacity than uplink. However, some use cases such as social networking, real-time video conferences and interactive applications have shown mostly symmetric traffic. Moreover, with the rise of 5G, various new use cases will be enabled. Tactile internet and applications in the ultra-reliable and low latency realm will require an optimization for both communication directions [16].

5G NR is an Orthogonal Frequency Division Multiplex (OFDM) scheduled system with a resource grid similar to LTE for a 15 kHz subcarrier spacing. The resource grid is comprised by subcarriers and OFDM symbols as shown in Figure 2.2. One resource element is comprised by a subcarrier and a OFDM symbol. Resources are shared dynamically depending on the user's traffic demands and channel characteristics in a way comparable to LTE [4].

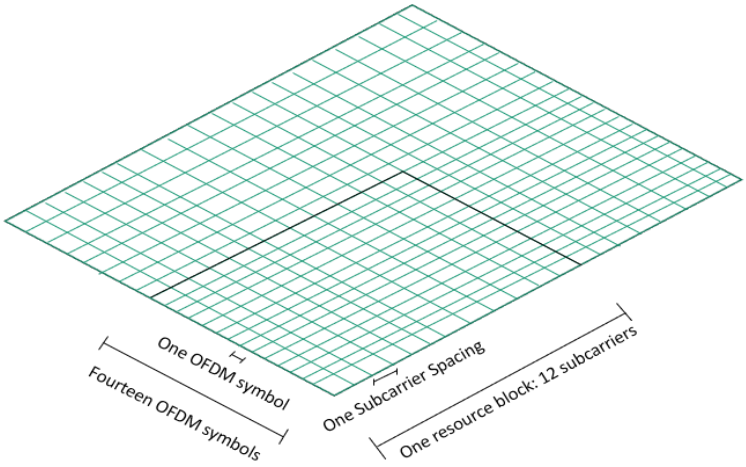

Figure 2.2: Time-Frequency Resource Grid for LTE/NR with subcarrier spacing: 15 kHz

One of the NR's main features is the usage of large number of antenna elements. In lower frequency bands, massive MIMO functionality allows for spatial multiplexing of user data

by beam forming, i.e. focus transmitted power into specific locations. However, beam forming serves an additional purpose at higher frequency bands such as the mmWave band due to its inherent propagation characteristics. They allow for narrower beamwidths and thus improve channel characteristics by increasing the received power and reduce interference [4].

Another important feature is the usage of multiple numerologies, i.e. in essence support different size of time-frequency resource elements [4]. These gives flexibility to NR by allowing it to support different types of services and also diverse frequency bands which may have different spectrum availability. NR scheduling is profoundly based on time, frequency, power and direction [4].

NR has adopted an ultra-lean design approach in order to maximize network efficiency. For instance, beam forming allows reference signals to be sent only to users that need them. In addition, NR sends synchronization signals with a periodicity of 20 ms which is 5 times frequent less than its LTE counterpart (4 ms) [4].

2.1.1 5G ARCHITECTURE

5G has been designed to support many diverse use cases. 3GPP has developed a novel system architecture for the radio access network (RAN) and core network (CN). In order to enhance scalability and maintainability, the new core network, 5G Core Network (5GCN), uses a service-based architecture. 5GCN splits control-plane/user-plane functions. The latter also means that you are able to scale the capacity independently for user-plane and control-plane functions. This architecture can be implemented with a physical node, distributed across many nodes, or on the cloud. All of these improvements give flexibility to the operators [4].

Another enhancement is the support for network slicing. Network slicing allows the creation of logical segments of the mobile network for particular businesses, use cases, i.e. one for conventional mobile broadband and one for critical industry-automation applications, or customers that need necessary network functions from the 5GCN service-based architecture [4].

The 5G NR logical radio access node is labeled as Next Generation Evolved Node B (ng-eNB), or abbreviated gNB. The gNB manages the radio resource management (RRM), routing of user-plane data to the User Plane Function (UPF), and control-plane information to the Access and Mobility Function (AMF), among others. The gNB is connected to the 5G core network via the NG interface. This interface is comprised by two subinterfaces NG-c and NG-u which connect to the AMF and UPF respectively. In addition, the Xn interface is used to connect gNBs between each other to support mobility and dual-connectivity.

Inter-rat mobility and quality of service handling in 5G is managed by the UPF. The AMF is responsible for control signaling between the core network and the device. As mentioned in the previous section, 5G NSA is based on using 5G NR and LTE simultaneously by using dual-connectivity. There are various combinations on how to connect the core networks and the radio access network of both RATs. Figure 2.3 illustrates Option 3 as the most appropriate for an early introduction of NR in existing networks.

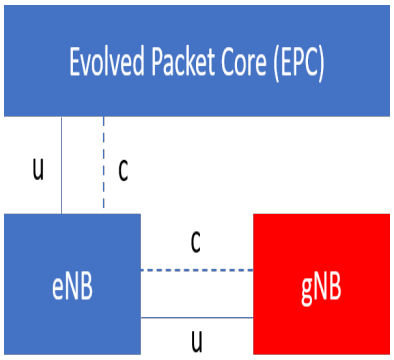

Figure 2.3: Option 3: Core Network and Radio Access Network for NSA [3]

With this setup, the gNBs will be connected to the Evolved Packet Core (EPC) via the legacy interfaces X1 which connects to the eNBs and this in turn to the Mobility Management Entity (MME) via the Xn interface. For NSA 5G, mobility is handled by the MME from LTE. For early deployments, non-standalone operation leverages the EPC to connect the NR radio access nodes and LTE access nodes. Figure 2.3 shows that LTE will be used for control-plane functionality and NR used for the user-plane.

2.2 LTE-NR INTERWORKING

Operators will commonly deploy NR as a high-frequency system for increased capacity. A high frequency system must be deployed in parallel with a low-frequency system in order to provide good coverage. The low-frequency system guarantees robust connectivity due to its inherent easier propagation characteristics, while the high-frequency system provides high capacity to achieve very high data rates [4]. For instance, in a multi-layer scenario, the macro layer would use a low-frequency high transmission power antennae, and the micro layer would use a high-frequency low-power transmitters with the advantage of having users closer.

5G NR is intended to build upon the already existing LTE infrastructure as it is a low frequency system. That means having a network layout with LTE-based macro cells and 5G-NR based micro cells. This type of network is known as an Heterogeneous Network. In NSA 5G, the user equipment is connected simultaneously to both LTE and NR as shown in Figure 2.4.

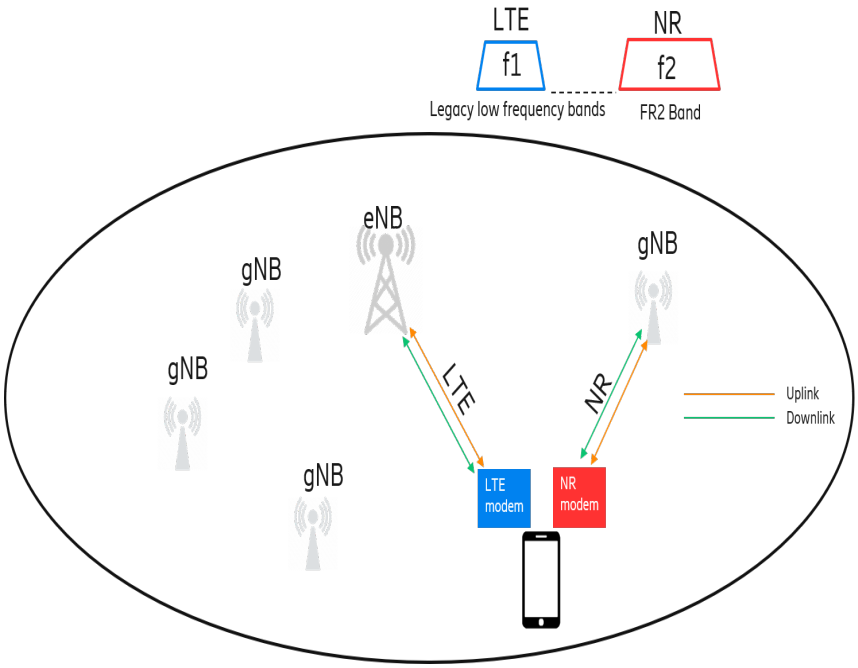

Figure 2.4: LTE/NR Dual-connectivity [4]

It is intended as well, to have co-sited deployments of LTE and NR, that may or may not

use the same spectrum. The latter is enabled by spectrum sharing technology, with yet again even more tight interworking as they are using the same spectrum giving an efficient solution for the operators as they don't have to lease/buy new spectrum. In addition, the idea is to morph the mobile network into NR-NR configurations with one of them using low frequency and the other high frequency. As shown in the Figure 2.6, the NR evolution is expected to progressively occupy low frequency bands that presently may be taken by other legacy wireless technologies [4]. 3GPP defined the Frequency Range 1 (FR1) band as the frequencies that range from 0.45 to 6 GHz and it also defined the Frequency Range 2 (FR2) band as those frequencies that range from 24.25 to 52.6 GHZ.

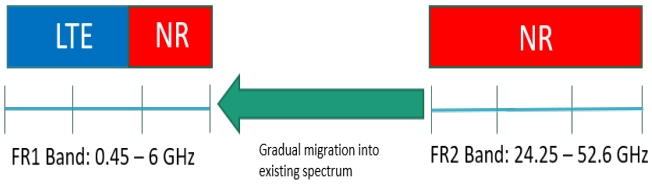

Figure 2.5: 5G NR evolution towards legacy bands

2.3 MULTI-CONNECTIVITY

MC, the general case for DC, is one key technology that will allow 5G to fulfill its full vision by improving user throughput, reliability and even enable ultra-reliable and low latency use cases. Multi-connectivity is defined as being connected simultaneously to multiple secondary access nodes from the same or different RAT. The master node manages the control-plane. As stated before, multi-connectivity is essential to provide robust connectivity when having mmWave cells, especially in urban city environments.

Carrier aggregation (CA), a technology in which the scheduler of a base station provides additional carriers for a user session, isn't possible across carriers of different radio access technologies. Therefore, DC has been standardized for NSA 5G [4]. With this setup, the serving access nodes of a particular user schedules its resources independently. CA and MC can be combined to have multiple carriers per connection and thus attain increased user throughputs. Coordinated Multipoint (CoMP) is another type of multi-connectivity solution intended to increase the throughput for cell-edge users.

It is important to note that MC indeed increases user throughput but it also increases interference on other nearby connections using the same frequency band (same frequency resources). Thus, in loaded scenarios, e.g. a dense urban city, multi-connectivity can hamper the user throughput by adding more interference if too many users are using the same frequency band. Moreover, if a user employs multi-connectivity using the same frequency band on its connections it employs intra-frequency MC. With intra-frequency MC, the connections interfere each other. Thus, to improve performance it is necessary to enable frequency diversity by having a deployment which uses various frequency bands. Having multiple connections using different frequencies (or RATs) provides increased user throughput, which is commonly known as inter-frequency MC.

Multi-connectivity has been studied extensively in the literature. The study in [17] proposes a multi-connectivity scheme that uses ultra-fast selection of serving cells from a set of prepared cells. With multi-connectivity the interruption from handover procedure is avoided because a set of serving cell(s), labeled as Active Set (AS), are prepared before transmission is broken. This schemes decreases the rate of radio link failures (RLFs), thus improving reliability. Multi-connectivity relies on this principle in order to reduce RLF for highly mobile users.

The study in [18] proposes a mobility context awareness algorithm to improve Quality of Experience (QoE) in traffic dense cellular networks. In this work, cell transition prediction is based on real-time geometry (log 10 of the received power and the interference power of adjacent base stations) measurements. In addition, it presents a vehicular cluster detection algorithm and it defines a threshold for geometry measurements, along with a traffic status indicator must indicate if there's enough data traffic demanded. It can proactively release resource blocks of the target cell and activate a small cell (for a data intensive vehicular cluster)..

The study in [19] presents a multi-connectivity mobility robustness optimization (MRO) algorithm that takes into account the basic mobility KPIs specified by 3GPP such as 1) Too late Handover (TLH) , 2) Too Early Handover (THE), 3) Handover to Wrong Cell (HWC) 4) Ping-pong effect. The implementation of the MRO is based on adjusting the handover threshold with a Corrective Indicactor Offset (CIO). These Key Performance Indicators (KPIs) are mapped to corrective indicators that indicate whether the CIO handover offset must increase or decrease. In addition, UEs are grouped based on the in-

formation of speed. Real-time tuning of CIO offset is done in every KPI period index. Results show that with the UE group specific MRO the cell updates on slow background UEs are reduced as compared to a cell-pair MRO leading to a 32% reduction. There's a full reduction of connection failures (or radio link failures) using multi-connectivity, but with a three-fold increase of signaling.

2.4 ULTRA-DENSE NETWORKS

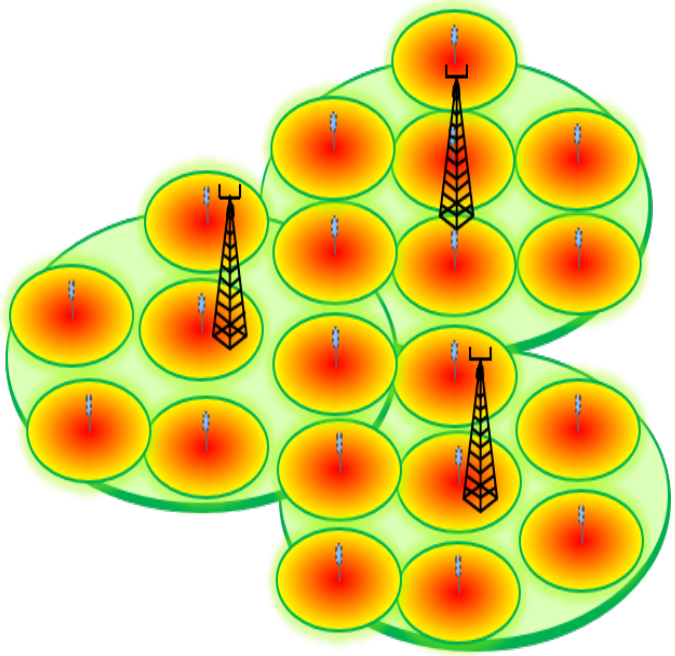

Figure 2.6: Ultra-Dense Networks

Ultra-dense networks mean having a much more dense deployments, even having more access nodes than actual UEs [20]. Ultra-dense networks fall under the umbrella of Heterogeneous Networks. These networks are comprised by using base stations of different coverage sizes, for instance having low power cells in combination with high power cells. However, the densification of access nodes also increases interference substantially particularly in downlink.

The survey in [20] provides an extensive literature review on modeling techniques of ultra-dense networks. In addition, it gives general guidelines on modeling path loss on UDNs, e.g. Rician Fading for Multipath Propagation. Modeling techniques range from

Game Theory and Stochastic Geometry. Poisson Point Process and Poisson Voronoi cells with Monte Carlo Method serve as tools to generate the probability density function of the size of the cells.

There are numerous studies on how to optimize RRM for such deployments in next generation networks. The study in [21] addresses 4 enablers for 5G RRM. First, interference management using other modulation scheme with beamforming on cell-edge users. Second, a dynamic traffic steering framework. Third, an Air agnostic Slice Enabler (AaSE), a network slice concept in NR, that uses Quality of Service (QoS) adaptation that influences user specific data flows to meet requirements of multiple slices served on shared resources. Fourth, it proposes the use of a common Packet Data Convergence Protocol (PDCP) layer for 5G and LTE.

Recently, since heterogeneous ultra-dense networks seem to be the deployment strategy for 5G rollouts, there has been numerous studies such as [22], that propose an architecture coupled with an UDN deployment. It proposes a dynamic traffic steering framework for increasing capacity, reliability and energy efficiency in the network. Its key proposal is dynamic QoS provisioning at the RAN. The access network is divided in Inner and Outer layer. Access Network - Inner (AN-I) layer steers low and high priority traffic, over low and high reliability links respectively. Access Network - Outer (AN-O) layer communicates with the core.

2.5 URBAN CITY ENVIRONMENTS MODELING

This section presents various approaches to model signal propagation in urban city environments.

This paper presents a cost-effective method to compute path loss in a city (streets). The model is called Berg Recursive Model, and it models diffraction when UE is in a non-Line-of-Sight (nLoS) position [23].

The study in [24] presents a fast method for computing micro and macro cell path loss in a realistic 3D urban city scenario for stationary and moving users. It proposes the usage of Rician Fading and free space path loss computation for UEs in Line-of-Sight (LoS)

with the base station, and Rayleigh Fading and Berg Recursive Model is used for UEs in nLoS. Conversely, geometry is used for path loss calculations of Macro-cells located in tall rooftops to model knife-edge diffraction.

[25] presents detailed guidelines on how to model an urban city scenario for system-level simulations for 5G. These guidelines propose the following approaches to model such urban scenarios:

- Map-based (e.g. Madrid Grid)
- Stochastic-based (Stochastic Geometry - Stochastic Deployments)
-Hybrid-based (Combination of deterministic and stochastic models)

The following document by ITU-R specifies guidelines [26] on how to model path loss in a wide plethora of scenarios: Dense Urban, Rural, Indoor Hotspot , Urban Micro, Urban Macro, Suburban Macro. A set of values for large scale parameters, delay line model and antenna radiation patterns as well.

From a realistic and practical point of view, the study in [27] establishes the following regarding coverage on urban city scenarios: Physical limits on power reception capabilities of antennae, radio frequency (RF) output power limitations and increased propagation losses are some of the challenges to provide coverage. Power levels and beamforming gains on the mid-band provide better coverage than its 1.8 GHz coverage. For high bands (around 30 GHz) outdoor coverage is achieved, but the Outdoor-to-Indoor (O2I) coverage is achieved utilizing planned deployments for LoS buildings that need to be covered. It establishes that eightfold improvements can be attained using 5G NR and LTE in terms of capacity and DL throughput.

Finally, the study in [28] also constructs a methodology for ultra-dense urban mmWave deployments by combining methods from queueing theory, stochastic geometry, ray-tracing and system-level simulations to create a comprehensive urban city scenario.

2.6 USER EQUIPMENT

Modern smartphones are becoming more and more complex. Presently, their main components are: a wireless connectivity system, a graphics processing unit, a central processing unit, an audio codec, a battery and interfaces towards the users, among others. These

components are depicted in Figure 2.7a. Historically, new radio access technologies have been able to increase the attainable user data rates at the cost of more power consumption on the UE [13].

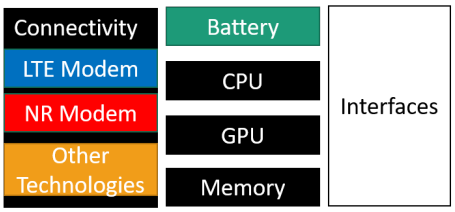

(a) High-level Components of a smartphone

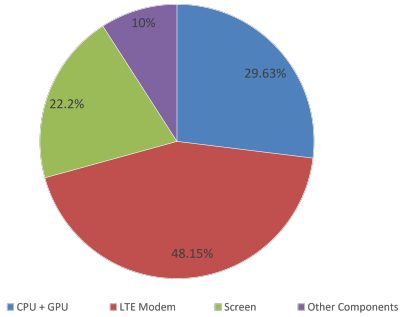

(b) Power consumption from a fully loaded LTE UE adapted from [29]

Figure 2.7: Smartphones' component power consumption breakdown

One of the main contributors for UE power consumption is the cellular subsystem, i.e. the LTE/NR modem, as shown in Figure 2.7b. And the modem's main power consumption contributor is the uplink transmit power [29]. The author in [30] establishes that there are multiple fronts to optimize power consumption on the cellular subsystem such as: power management controlled by the device's Operating System (OS), chipset design and network-controlled mechanisms such as scheduling, power control and mobility management. Our study focuses on saving UE power consumption via mobility management when using multi-connectivity within an ultra-dense network deployed in a urban city environment.

Figure 2.7b illustrates that the modem power consumption is responsible for 48% of the UE's total power consumption. In addition, from this percentage the uplink transmit power is responsible for half of the modem's power consumption according to [29]. How-

ever, the study in [31] points out that the distribution of the modem's power consumption might shift to baseband processing as the largest contributor due to the envisioned extreme data rates.

Gene's law, an extension of Moore's law, establishes that the power consumption for the same performance is halved every 18 months [30]. It is uncertain how the power consumption of the NR device will evolve as 5G matures, nonetheless the same study estimates that the 5G receiver will achieve a power consumption level similar to LTE as of 2014 in 2027 [31]. The UE power consumption model employed in our study is mainly dependent on the uplink transmit power and it will be described in the Implementation section of the report.

2.6.1 UE CHANNEL SOUNDING

In order to exchange useful data, the user equipment and the base stations must be able to have knowledge of the radio channel characteristics over which user data is sent. This information is obtained via measurements of reference signals on the receiver or on the transmitter side. Following ultra-lean design principles, 5G NR intends to avoid "always ON" signals as much as possible to save energy both on the base stations and on the user equipment.

Channel State Information - Reference Signal (CSI-RS), a type of reference signal, can be sent in an aperiodic manner to assess the downlink channel. The Synchronization Signal (SS) block is the only reference signal that must be transmitted periodically [4]. The SS block helps the NR devices find a cell when entering the coverage area of a system [4]. Similarly, the uplink is assessed via the Sounding Reference Signals (SRS).

After the UE has sounded the channel, comes the reporting of the measurements to the network. These are some of the reported quantities:

-CQI (Channel Quality Indicator) - mainly used for scheduling

-RSRP (Reference Signal Received Power) - used for handover, beam management and radio resource management.

-SINR (Signal-to-Interference plus Noise Ratio) - used for handover.

The latter takes into account the received power and the interference levels and thus it is a useful measurement for ultra-dense heterogeneous deployments. This measurement will be used throughout our study. Handovers in our simulations are based on the DL SINR. In addition, radio link failure (RLF), a state in which the user is unable to transmit or receive data, is triggered below a specific low DL SINR. Moreover, the DL SINR is used as a secondary cell association criteria for the baseline multi-connectivity scheme used in this work detailed in Section 5.

2.6.2 RRC STATES

The UE can be in different radio resource control (RRC) states depending on the user traffic activity. Users in current mobile networks can be in one of this RRC states: RRC IDLE and RRC CONNECTED. In 5G NR, a third RRC state called RRC INACTIVE was defined. This state was initially developed and proposed in [32]. Its purpose is to be efficiently reachable by the mobile network and quickly start transmitting data with minimum signaling overhead.

As this study concerns scenarios when the user is transmitting/receiving data with traffic scenarios with few user transitions, energy consumption on state transitions is considered negligible. Thus, only Idle and Active RRC states are included in our system level simulations. The following power states were used for the different RRC states to model the power consumption of the terminal. In the context of NR, RRC IDLE can be seen as being in Micro Sleep Power State and RRC INACTIVE can be seen as being in Idle Power State. Figure 2.8 shows the user RRC states mapped to their corresponding possible power states. The user power states will be described in Section 5.

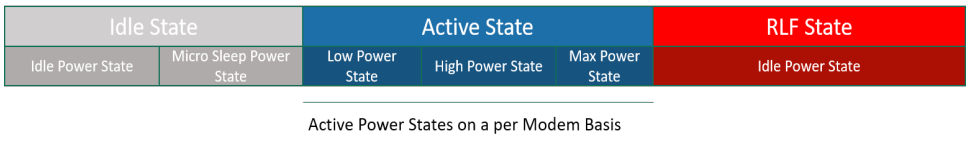

Figure 2.8: RRC states mapped to its possible Power States.

2.6.3 UPLINK POWER CONTROL

This subsection addresses the uplink power control mechanism employed in 5G. Uplink power control "is the set of algorithms by which the transmit power for different uplink physical channels and signals is controlled in order to ensure they are received by the network at an appropriate power level" [4]. NR uplink power control builds upon the existing power control framework , based on open-loop and closed-loop, with some additional extensions to beam-based power control [4].

There are two types of uplink power control mechanisms:

- Open-loop: estimate the channel's path loss according to DL measurements. It can be performed with fractional or full path loss compensation.

- Closed-loop: when the networks informs the UE about its uplink received power and executes power control commands if the desired power level isn't reached.

The study in [33] derived the most well-rounded parameters for uplink power control which we used for our work. In addition, we use a fractional open-loop power control mechanism as shown in Eq. 2.1.

$$P_{PUSCH} = min\{P_{CMAX}, P_0 + \alpha PL + 10\, log_{10}(M)\} \tag{2.1}$$

Where M stands for the number of resource blocks, P_0 for the target received power, P_{CMAX} stands for the maximum uplink transmit power per carrier, α a network configurable parameter related to fractional path-loss compensation and PL accounts for the pathgain and P_{PUSCH} stands for the uplink transmit power per carrier. $PUSCH$ stands for the Physical Uplink Shared Channel.

In uplink, the resources are power limited. Power availability is reported to the network via the Power Headroom Report (PHR) , and its current NSA operation power availability is prioritized to LTE [4]. The reasons to allocate power as efficiently as possible are twofold. Firstly, the transmit power per uplink carrier is limited by the device's power class. Secondly, there's a maximum total transmit power across all carriers due to regulatory reasons [34].

2.7 RELATED WORK

This section is subdivided into energy saving mechanisms for the UE and multi-connectivity schemes that target power consumption reduction on the UE. Reliability studies using multi-connectivity are also included in this section.

2.7.1 ENERGY SAVING MECHANISMS FOR THE USER EQUIPMENT

In current state-of-the-art technology, numerous mechanisms exist to save energy on the user equipment to improve energy efficiency and save battery power consumption. Some are implemented in the network and others are implemented in the user equipment.

For instance, in 2G, voice activity detection mechanisms were used to detect when a user wasn't speaking and then decide to turn off the UE during these periods in order to save energy. Similarly, subsequent 3G and 4G releases included Discontinuous Reception (DRX) in their specifications [35]. DRX is a mechanism in which the device periodically switches to active mode to monitor the Physical Downlink Control Channel (PDCCH) to check if it's being scheduled, and after the ON period has passed, it immediately goes into sleep mode, will also be included in NR [4]. These improves battery consumption at the cost of increasing latency. DRX has been studied extensively in the literature. The study in [36] shows that energy savings due to extended DRX cycles range from 10-20% when the device is transmitting frequently.

In 5G NR, one of the standardized power-saving mechanism on the NR device is receiver-bandwidth adaptation. Essentially, with this mechanism, the user equipment uses less bandwidth to monitor control channels, and a wide bandwidth to receive data [4]. Moreover, 5G NR has been designed to follow ultra-lean design principles and thus it has various energy saving mechanisms tailored for the user equipment and in addition MTC devices. As mentioned in Section 2, gNBs now sends synchronization block signals (SS), used to allow NR devices to discover the network, with a periodicity of 20 ms which is 4 times sparser than in LTE (4 ms). Moreover, with the advent of beamforming it is possible to transmit SS blocks in a time-multiplexed fashion to specific users which improves network and UE energy performance [4].

The study in [37] presents a DRX model for 5G system level simulations with 4 and 5-state semi-Markov model. Performance of both setups are analyzed with a bursty data traffic model in terms of the inactivity timers, showing a DRX model with 5 states with superior results in terms of both power saving factor and delay. Another reason why a new RRC state in NR has been standardized.

The study in [38] proposes an algorithm that assigns UEs to different eNBs, that is, minimize the number of UEs per eNB to maximize performance. The study in [35] provides a wide range of recommendations to ensure an energy efficient 5G UE. Among those recommendations which stand out are: "1. The design of energy efficient wake up and re-synchronization methods." "2. Better energy efficiency can be achieved using a combination of high data rates and low power sleep modes." This fact in particular is one way multi-connectivity can improve energy efficiency and our study addresses this aspect.

In the context of mobile edge computing (MEC), the study in [39] proposes an energy-efficient computation offloading scheme for single-frequency heterogeneous networks. Depending on the delay constraints of the computation task and the interference on the network, the authors propose a scheme that optimizes the energy consumption of both the UE and the MEC server. The scheme attains an average 18% decrease in energy consumption on the device compared to not offloading. Similarly, [40] studies a "cyber-foraging" approach in which the user equipment is constantly searching for computing resources on the edge. The latter prolongs battery life of the user equipment by offloading the computation tasks of the end-user applications. However, this approach can only be done for non-interactive applications due to the relatively high latency.

In addition from the network's point of view, power-saving techniques have been a priority since the energy consumption of the network directly reflects on the operational costs for the operators. The study done in [41] investigates specific techniques to reduce energy consumption at the site level. This paper proposes the following techniques: 1. Using shared power amplifiers (PA) for multi-RAT radio base stations (RBSs). 2. Load Balancing from LTE to High Speed Packet Access (HSPA) when low data traffic is required.

2.7.2 MULTI-CONNECTIVITY SCHEMES

The study in [5] establishes that carrier aggregation (CA) has a positive effect in the UE power consumption as long as it boosts the DL data rate by at least 25%. In fact, the UE Power Consumption Model for carrier aggregation defined in this work is extended from this study. The work in [42] studies the effects of decoupling uplink and downlink. Its main premise is to use path loss as an uplink handover criteria, in order to offload traffic from macro cells to the much closer small cells. This yields a reduced uplink transmit power, and improves uplink SINR thus improving uplink throughput.

The work done in [43] presents a comprehensive survey of mobility management in the context of heterogeneous networks for Long Term Evolution - Advanced (LTE-A). It showcases a plethora of handover decision algorithms based on optimizing SINR and reduce energy expenditure. Particularly, it describes two categories for handover algorithms: cost-function based and energy efficient. Cost-function based can be based on battery lifetime, traffic type and cell load. This study defines energy efficient algorithms for the UE as those that minimize interference.

The study in [44] introduces a novel energy-centric handover decision scheme based on minimizing UE power consumption. It employs an adaptive hysteresis margin that favors an adjacent cell with good path loss and low interference. The latter shows gains in energy efficiency by up to 88% compared to a strongest cell handover scheme. The study in [45] proposes a handover decision algorithm based on multiple criteria to execute a handover: RSRP, UE transmit power and cell capacity. Simulation results show that the proposed scheme can save up to 50% in UE transmit power compared to a conventional strongest cell handover scheme.

The study done in [46] proposes a series of MC schemes to improve performance on the network side. One of his proposed MC schemes, BEST SINR, is used as a baseline MC scheme in our work, to assess the performance of the user equipment. This scheme will be described briefly in Section 5.

3 METHODOLOGY

Throughout our work, we based our study on the methodology diagram described in Figure 3.1. This diagram presents the research workflow from the problem statement up to the publication of a research paper.

First, we defined our problem statement. After we narrowed down the problem statement, we performed multiple literature reviews to define our scenario. Thereafter, based on our scenario, we leveraged theoretical models from the literature and adapted them to our needs or proposed our own. Thereafter, we implemented these models and integrated them into the simulator. For each implemented model, we performed simulations and modified the platform accordingly to integrate and validate each model separately. The same process applies for the algorithms that we designed and implemented in our work.

Our simulations followed the framework described in [47] and it involves iteratively modifying the platform and analyzing the results until the scenario is validated. After the simulations were revised, we evaluated our results. If necessary the scenario was redefined in order to attain valid results. Finally, we concluded based on our results and we answered the research questions defined in our work. Thereafter, this results will lead to a publication of a research paper on a conference and/or journal.

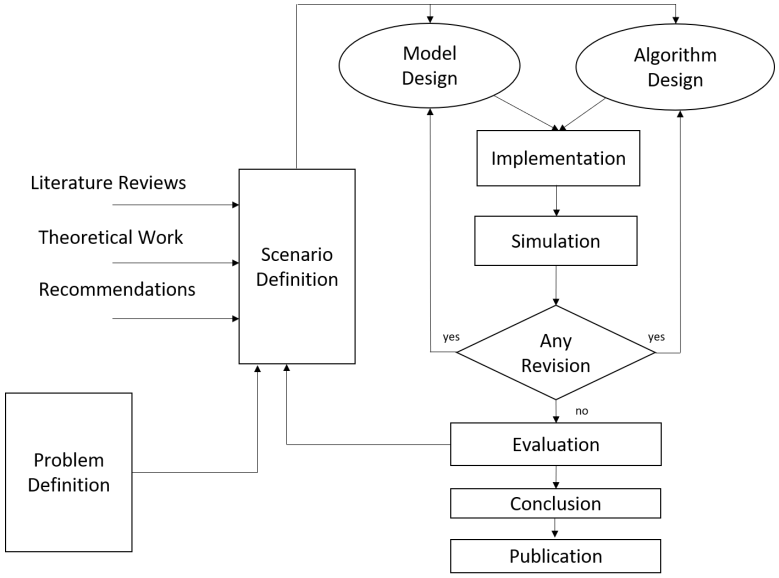

Figure 3.1: Research Methodology

4 THEORY

This section addresses the usage of multi-connectivity within an ultra-dense network and likewise the metrics to study the performance of the user equipment. Subsection 4.1 encompasses relevant concepts in an ultra-dense network. Subsection 4.4 addresses the metrics to study UE performance.

4.1 MEASUREMENTS AND INTERFERENCE

Ultra-dense networks are an important solution to address the ever-increasing data demand. One of its main challenges is the substantial increase in interference. Hence, one important channel measurement is the Signal-to-interference-plus-Noise-ratio. This measurement is defined as the power of the received signal divided by the sum of the interference power and noise as shown in Eq. 4.1.

$$SINR_{DL} = \frac{Pt_{BTS \to UE} \cdot G_{BTS \to UE}}{\sum_{BTS_i \subseteq BTS_{RAT}} Pt_{BTS_i \to UE} \cdot G_{BTS_i \to UE} + N_0} \tag{4.1}$$

Eq. 4.1 corresponds to the SINR experienced by a user, referred to as the DL SINR, where P_t is the transmit power of the BTS , $G_{BTS \to UE}$ is the downlink channel pathgain, N_0 is the noise term, BTS_{RAT} corresponds to the BTSs using the same radio access technology/frequency. The first term in the denominator is the interference term. It corresponds to the interference caused by other cells transmitting useful data to its users, referred to as inter-cell interference. In an ultra-dense network, this kind of interference increases substantially due to the increased number of access nodes and also since nodes are so close to each other.

$$SINR_{UL} = \frac{Pt_{UE \to BTS} \cdot G_{UE \to BTS}}{\sum_{UE_i \subseteq UE_{RAT}} Pt_{UE_i \to BTS} \cdot G_{UE_i \to BTS} + N} \tag{4.2}$$

Similarly, Eq. 4.2 describes the SINR experienced at the base station, known as the UL SINR. In this case the $G_{UE \to BTS}$ is the uplink channel pathgain, P_t is the UE transmit

power and UE_{RAT} corresponds to the UEs transmitting on the same frequency. The UL SINR is the power of the received signal transmitted by the relevant user divided by the interference power of other users transmitting data to adjacent cells. The uplink interference increases substantially as the load increases.

Since LTE and NR are both an OFDM scheduled system, users connected to the same cell don't interfere with each other since the channels are orthogonal. It applies for both uplink and downlink. In an UDN scenario, i.e. having more base stations than users, the downlink interference is typically higher than its uplink counterpart due to the increased number of downlink reference signals in an ultra-dense network and the high probability of having other access nodes nearby. In a dense loaded scenario, uplink interference is typically higher since it's more probable to have users closeby transmitting in uplink.

When users employ multi-connectivity, a new interference term may appear in the denominator. This kind of interference occurs when two or more of the cells the user is connected to use the same frequency which is known as intra-frequency multi-connectivity. This generally happens when they are using the same radio access technology with a single spectrum allocation. Hence, employing multi-connectivity with frequency diversity in a heterogeneous deployment can avoid this term. The downlink interference for a particular connection due to multi-connectivity can be described as shown in Eq. 4.3.

$$I_{MC,DL} = \sum_{BTS_i \subseteq AS_f} Pt_{BTS_i \to UE} \cdot G_{BTS_i \to UE} \tag{4.3}$$

Where AS_f is the active set of connected cells that use the same frequency. This type of interference also happens in uplink. For instance this kind of interference happens if a user is connected to an LTE cell and two NR cells operating at the same frequency. The NR cells interfere each other. The same happens for the uplink. Essentially, the user's connected master cell and secondary cells interfere each other if they use the same frequency. Eq. 4.4 and 4.5 show the new terms for UL and DL SINR if the user employs intra-frequency multi-connectivity. It is important to note as well that the usage of multi-connectivity increases the first interference term for other users connected on different cells using the same RAT.

$$SINR_{DL} = \frac{Ptx_{BTS \to UE} \cdot G_{BTS \to UE}}{\sum_{BTS_i \subseteq BTS_{RAT}} Ptx_{BTS_i \to UE} \cdot G_{BTS_i \to UE} + I_{MC} + N} \tag{4.4}$$

$$SINR_{UL} = \frac{Ptx_{UE \to BTS} \cdot G_{UE \to BTS}}{\sum_{UE_i \subseteq UE_{RAT}} Pt_{UE_i \to BTS} \cdot G_{UE_i \to BTS} + I_{MC} + N} \tag{4.5}$$

4.2 UPLINK BEHAVIOR

As shown in Figure 4.1a , the uplink power control follows the pathgain and adjusts the uplink transmit power accordingly to meet a target received power at the base station. This is the main function described in Eq. 2.1 from Sec. 5.6.

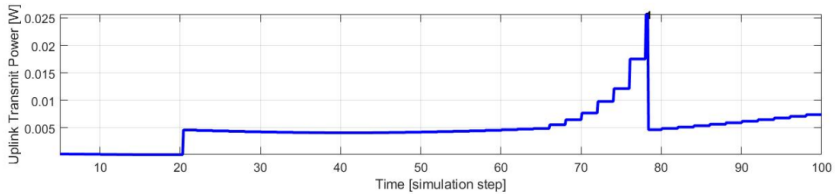

(a) Uplink Transmit Power for a User

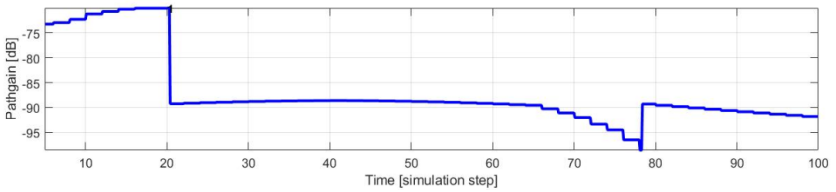

(b) Pathgain experienced by a User

Figure 4.1: Uplink Power Control illustration for a single uplink carrier using Single-connectivity

The effect of the uplink power control mechanism on the user transmit power is captured in Figure 4.1a. Note that the user executes two handovers (at simulation step = 20 and at simulation step = 78) as the abrupt changes in uplink transmit power indicate. Note that the handover criteria for our system is based on the DL SINR. Section 5 will describe the system model in detail.

4.3 USER FLOW

In this section we are going to exemplify the typical behavior of a user in our system. We are going to display the UE Power Consumption as a function of time. Let's suppose the user needs to transmit three 5 MB file. Figure 4.2 portrays the evolution of the UE power consumption when transmitting three files with different connection setups. First the user employs single-connectivity (SC) for the first file, then dual-connectivity for the second file and afterwards tri-connectivity (TC) for the third file. The green lines symbolize the variability of the active UE power consumption when the user is in ACTIVE mode. This variability is dependent on the radio conditions experienced on each connection.

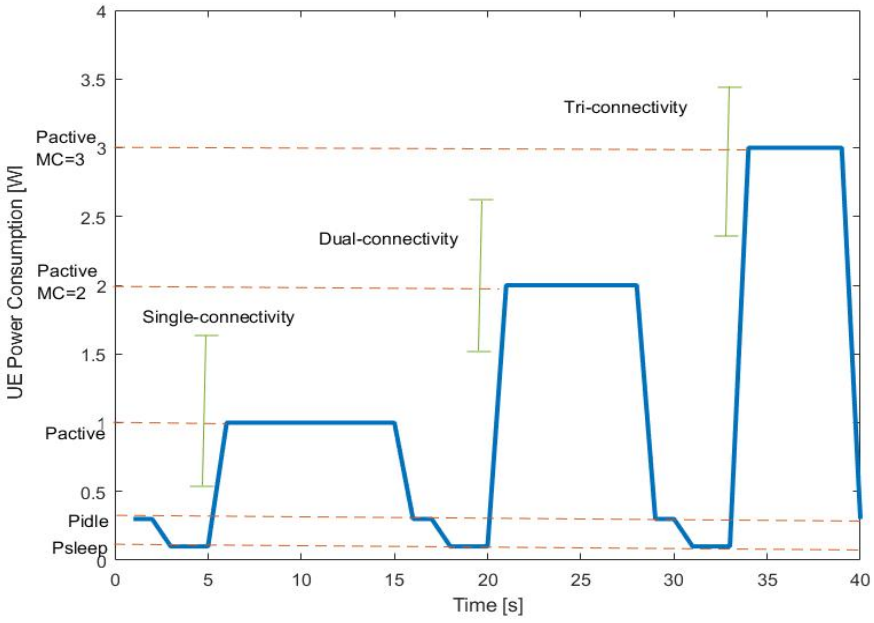

Figure 4.2: Typical UE Power Consumption in a Multi-connectivity scenario

To our understanding, there are two paths to achieve UE energy efficiency: One of them is to minimize UE power consumption when the user is in ACTIVE Mode. The other approach is based on minimizing time the users spend in ACTIVE mode.

For the former, one approach would achieve this task by avoiding the high transmit power region on the UE. For instance, a secondary cell association scheme based on targeting an upper bounded minimum uplink transmit power. For the latter, an approach that maximizes uplink and downlink throughput, so that users can switch to IDLE mode (sub-

sequently to micro sleep) as quickly as possible. Section 5 will describe the UE power consumption model in detail.

4.4 METRICS

This subsection describes the metrics used in this study. This work studies UE performance in terms of user throughput, power consumption, energy efficiency and reliability. User throughput, commonly measured in [Bits/s], can be divided into downlink and uplink throughput. There are many factors that influence the experienced user throughput. The Shannon-Hartley Formula as shown in 4.6 and 4.7 is one common approach to estimate user throughput. The downlink and uplink throughput estimation given by the Shannon Formula are shown in Eq. 4.6 and 4.7 respectively.

$$R_{DL} = BW_{DL} \cdot log_2(1 + SINR_{DL}) \tag{4.6}$$

$$R_{UL} = BW_{UL} \cdot log_2(1 + SINR_{UL}) \tag{4.7}$$

As explained in Section 2, multi-connectivity increases user throughput by essentially aggregating additional capacity to users. Now, the downlink throughput is given by the Eq. 4.8. Similarly, Eq. 4.9 describes the uplink throughput for multi-connectivity.

$$R_{DL} = \sum_{BTS_i \subseteq AS} BW_{BTS_i,DL} \cdot log_2(1 + SINR_{BTS_i,DL}) \tag{4.8}$$

$$R_{UL} = \sum_{BTS_i \subseteq AS} BW_{BTS_i,UL} \cdot log_2(1 + SINR_{BTS_i,UL}) \tag{4.9}$$

Another metric of interest for our studies is the power consumption of the device. Power consumption, typically measured in Watts [W] or milli-Watts [mW], is given by empirical models dependent on specific parameters.

Energy efficiency is another useful metric. The energy efficiency (EE) in the context of wireless networks, is the transmission and/or reception of bits per unit of energy [Bits/J]. For the user equipment, the UE energy efficiency can be subdivided into downlink EE

and uplink EE, or defined as a global energy efficiency which takes into account both communication directions. The global UE energy efficiency is given by the Eq. 4.10.

$$\overline{EE}_{UE} = \frac{\overline{R}_{DL} + \overline{R}_{UL}}{\overline{P}_{T,UE}} \tag{4.10}$$

Since we are concerned with the energy efficiency of an individual UE, we compute the average UE energy efficiency using multi-connectivity. Although, a similar behavior might be observed if we calculate the system energy efficiency, considering all UEs as a system. The UL UE energy efficiency is given by Eq. 4.11 and the DL UE energy efficiency is given by Eq. 4.12.

$$\overline{EE}_{UE,UL} = \frac{\overline{R}_{UL}}{\overline{P}_{T,UE}} \tag{4.11}$$

$$\overline{EE}_{UE,DL} = \frac{\overline{R}_{DL}}{\overline{P}_{T,UE}} \tag{4.12}$$

In this study we study reliability in terms of mobility. We use the radio-link failure (RLF) rate as a quantitative metric to assess reliability. RLF rate is defined as the time the user spends in RLF state divided by the total simulation time.

5 IMPLEMENTATION

This section describes the system models that comprise this study. Subsections 5.1 and 5.2 provide the details on the construction of a dense urban city model and the propagation models used to model legacy and mmWave communication. Subsections 5.3, 5.5 and 5.6 describe the UE power consumption model, the multi-connectivity framework. the uplink power control scheme for multi-connectivity, and a multi-connectivity scheme proposed in this work.

5.1 URBAN CITY MODEL

In our work, we integrated an urban city environment that captures the intricacies of mmWave propagation based on the ITU-R M.2135 propagation model. This urban environment is based on what is known in the literature as the Manhattan Grid. The Manhattan Grid is comprised by multi-story buildings and streets. The network deployment used in our work is comprised by LTE macro cells located at the rooftops of the buildings, and NR small cells deployed on the streets.

The network deployment is shown in Figure 5.1. The NR cells deployed in the streets mimic small antennae deployed on traffic lights and the LTE cells correspond to a typical way macro cells are deployed in current mobile networks. The NR base stations are placed very densely in the urban environment and thus create an ultra-dense network. As described in Section 2.5, METIS's simulation guidelines defined three main approaches to model a dense urban city scenario: stochastic, hybrid and map-based [25]. In this work, we chose the map-based Manhattan Grid as the city layout comprised by multi-story buildings and streets. The urban city layout is described in Table 5.1.

The parameters for the ultra-dense network deployment are shown in Table 5.2. The ultra-dense network is comprised by three deployment tiers. The first tier is the LTE macro tier operating at 2 GHz. The second tier is comprised by NR small cells operating at 28 GHz labeled as NR_1. The third tier is comprised by another NR deployment of small cells operating at 26 GHz labeled as NR_2.

Table 5.1: City Layout

City Layout	
Building Height	12 m
Street Width	20 m
Building Width	40 m
Number of Horizontal Streets	11
Number of Vertical Streets	11
Total Number of Buildings	100
Floors per Building	3
Floor Height	4 m

Table 5.2: Network Deployment Parameters

Network Parameters			
RAT	LTE	NR (NR1)	NR (NR2)
Frequency	2 GHz	28 GHz	26 GHz
Carrier Bandwidth	40 MHz	40 MHz	40 MHz
Antenna Height	22 m	10 m	10 m
Antenna Type	Tri-sector	Omni	Omni
Intersite Distance	272.12 m	69.72 m	69.72 m
Carriers per Connection	1	1	1
Number of Sites	9	61	61

5.2 PROPAGATION CHARACTERISTICS

It is expected that early 5G rollouts will take place primarily in dense urban cities in order to enable the initial eMBB use cases. Moreover, the uplink transmit power is primarily dependent on the channel's radio conditions. In this work, special attention is taken to accurately model mmWave and low frequency propagation in urban environments. Via field measurements on FR2 frequencies, METIS-I proposed a modified version of the ITU-R M.2135 propagation model to adapt it to the FR2 frequency band [48]. In this study, we employ the aforementioned path loss model for Urban micro (UMi) scenarios at 28/26 GHz for LoS and nLoS communication.

The open source code developed in METIS project was modified in order to match the field measurements for such frequencies. For the FR1 frequency band, we used the Urban Macro (UMa) propagation model defined in [25] for urban environments. Both of these propagation models are based on the original ITU-R M.2135 defined in [26]. Figures 5.2a and 5.2b illustrate the propagation characteristics for both RATs at such frequencies. The

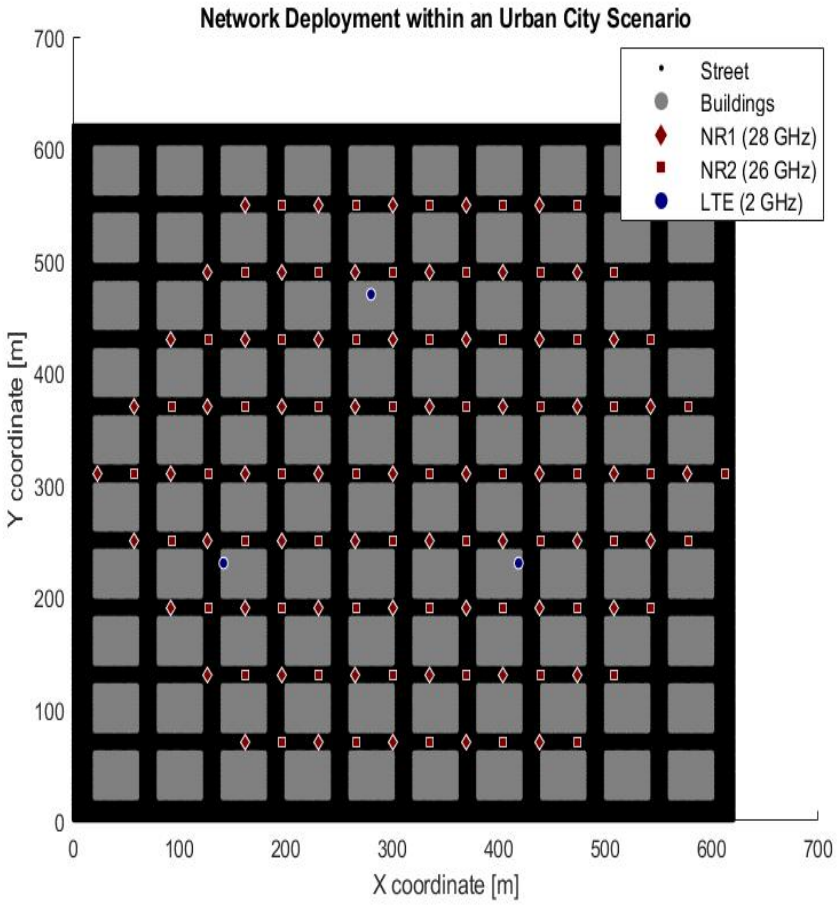

Figure 5.1: Network Deployment within the Manhattan Grid

propagation characteristics at 26 GHz are similar to 28 GHz.

Evidently, the propagation characteristics for the FR1 and FR2 bands are distinct. For the former, the model takes into account the scattering objects in the environment, i.e. multi-story buildings, and thus most part of the signal reaches the users via diffraction. For the latter, higher indoor penetration loss and low diffraction yield a tough environment for nLoS. You can find other parameters used for both propagation models in Table 5.3. The reader can refer to Appendix 1. for more details about the propagation models employed in our work.

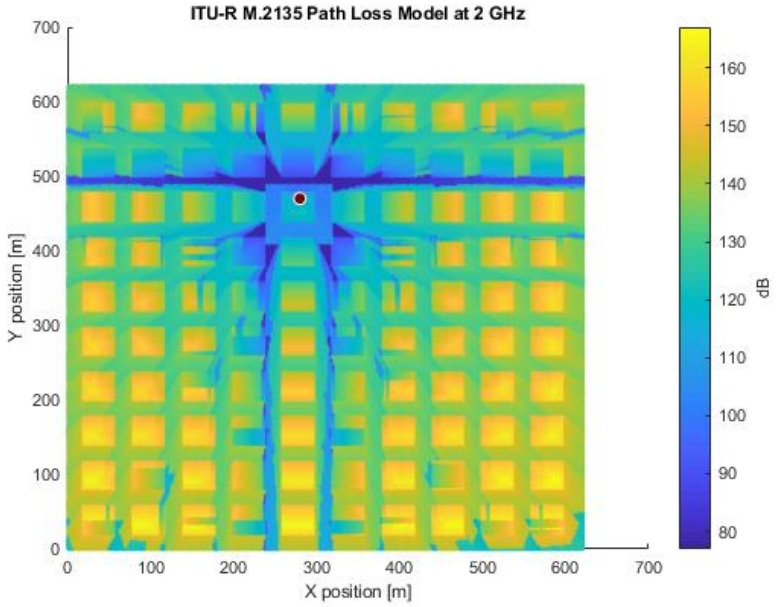

(a) Path Loss Map for a LTE macro base station

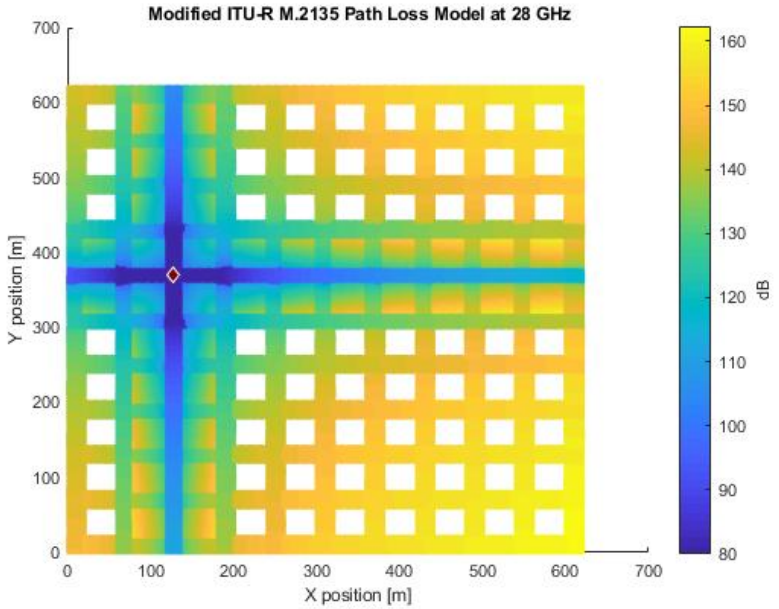

(b) Path Loss Map for a NR micro base station

Figure 5.2: ITU-R M.2135 at 2 GHz and Modified ITU-R M.2135 at 28 GHz.

Table 5.3: Parameters for the Path Loss Models used for LTE and NR

Parameter	LTE	NR
Path Loss Offset	–	10 dB
Log-Normal Shadowing std	8 dB	8 dB
Minimum Coupling Loss	77 dB	80 dB

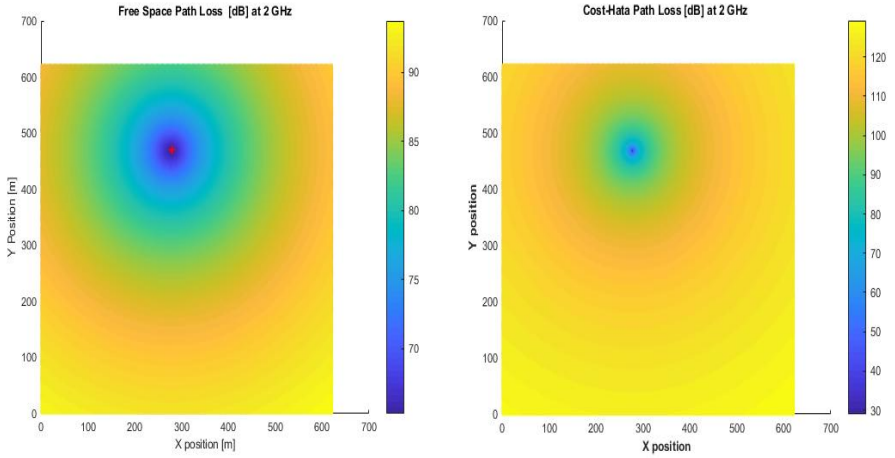

(a) Free Space Path Loss at 2 GHz for a single BTS located at x = 280 m, y = 470 m

(b) Cost-HATA Path Loss at 2 GHz for a single BTS located at x = 280 m, y = 470 m

Figure 5.3: Comparison of Simple Propagation Models

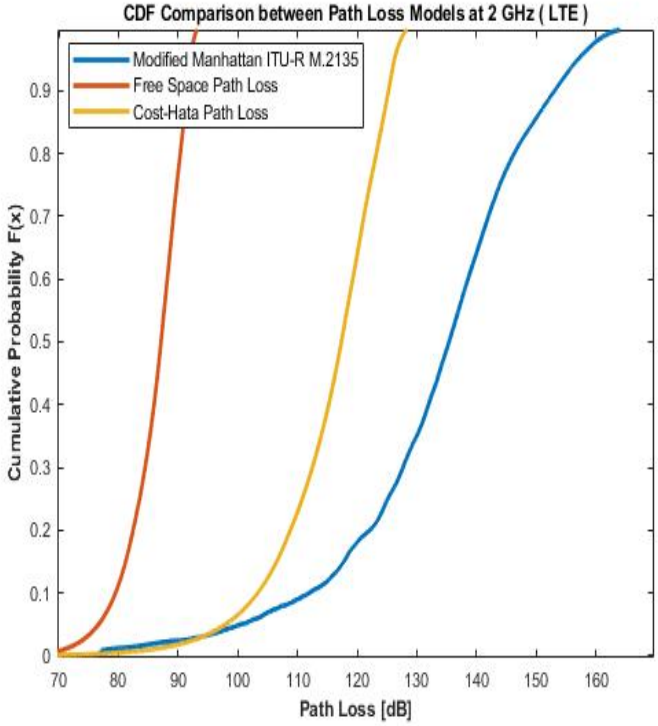

Figure 5.4: CDF Comparison between Path Loss Models at 2 GHz for a single BTS located at x = 280 m, y = 470 m

The Log-Normal slow fading std is chosen as 8 dB in order to take into account other scattering objects that might be present in an urban environment. The Cumulative Distribution Function (CDF) between the COST-Hata Propagation model, Free-Space Propagation Model and the ITU-R M.2135 at 2 GHz, shown in Figure 5.4, illustrates the effect of an urban environment. This is one evidence that shows that the link budget is reduced on city scenarios. Since the free-space propagation model and Cost-Hata propagation model aren't suited for mmWave frequencies, these models weren't compared with the ITU-R M.2135 at 28 GHz from METIS.

5.2.1 USER CREATION AND MOBILITY MODEL

Throughout the simulations in this study, users are created statically. Users are created randomly within vertical or horizontal streets and close to the network deployment. Users are able to move north and south if they are created on a vertical street. At the beginning of the simulation, users have a 50% probability of heading north or south if they are created on a vertical street. Similarly, users created on a horizontal street have an equal chance to move east or west.

An imaginary circle encloses the network deployment. When users are close to the edge of the deployment they bounce on this imaginary circle and head to the opposite direction. This mobility model can be used to model fast-moving cars and slow-moving pedestrians. Throughout the simulation, the users always remain outdoors. Figure 5.5 illustrates the movement of the users throughout the simulations.

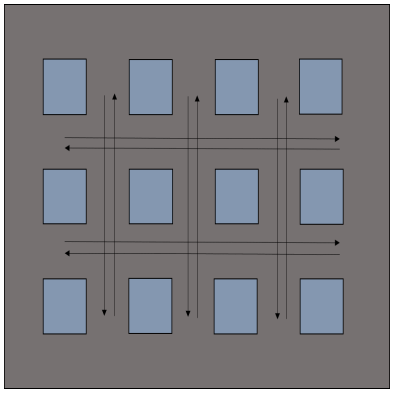

Figure 5.5: Mobility Model for the Urban City scenario

5.3 UE POWER CONSUMPTION MODEL

NSA operation will require NR devices to have both 4G and 5G chipsets, especially if both RATs are used in very distinct frequencies. Moreover, as low frequency LTE spectrum is gradually migrated into 5G, multiple chipsets may be required for the 5G evolution as well. The study in [49] proposed a context-aware UE power consumption model dependent on the uplink transmit power and on carrier aggregation. The device-under-test (DUT) is an LTE-A Cat-6 device from year 2016, given from the study in [5].

In our work, we used this model and extended it for downlink power consumption with recommendations provided by the authors of this study. The total UE power consumption when the user is ACTIVE is divided in two parts: a) UE power consumption due to uplink and b) UE power consumption due to downlink. The total UE power consumption is given by Eq. 5.1.

$$P_{T,UE} = m_{ACTIVE} \cdot (m_{DL} \cdot P_{UL} + m_{UL} \cdot P_{DL}) + m_{IDLE} \cdot \overline{P}_{\{0,1\}} \tag{5.1}$$

where:

P_{UL} = power consumption due to uplink
P_{DL} = power consumption due to downlink
m_{ACTIVE} = boolean variable for ACTIVE RRC state
m_{IDLE} = boolean variable for IDLE RRC state
m_{DL} = boolean variable if the UE has data to receive on its downlink buffer
m_{UL} = boolean variable if the UE has data to transmit on its uplink buffer
$\overline{P_0}$ = Micro Sleep Power State
$\overline{P_1}$ = Idle Power State

The model dynamically evaluates the power consumption depending on the communication direction of the user at any given time. For instance, if the user has data only on its uplink buffer, then the user is in ACTIVE mode and transmitting data. In this case, m_{ACTIVE} and m_{UL} are set to one and the other boolean variables are set to zero and thus the model takes into account the P_{UL} until the uplink buffer is empty. Section 5.3.1 describes in detail the power consumption contribution for data transmission in uplink.

The model evaluates P_{DL} in a similar fashion if the user is only "scheduled" in downlink. Section 5.3.2 does the same for data reception in downlink. If the user is transmitting and receiving data simultaneously then the total UE power consumption is the sum of P_{UL} and P_{DL}.

If both downlink and uplink buffers are empty for more than 100 ms the user switches to RRC IDLE state. Within this RRC state, the user can be on two global power states. Idle Power State ($\overline{P}_1$) when the user has recently switched from another RRC state, and Micro Sleep Power State ($\overline{P}_0$) if the user has been in IDLE mode for more than 100 ms. Note that the Idle and Micro Sleep Power states are global and not per link direction or connection. In our simulations, we record the power consumption of the user equipment throughout the duration of the simulation.

5.3.1 UE POWER CONSUMPTION DUE TO THE UL

The relationship between the UE power consumption and the uplink transmit power is given by a piecewise function with device-specific parameters shown in Eq. 5.2 [49]. The α and β parameters are derived empirically by measuring the power consumption of the user equipment for different uplink transmission powers. The curve has two regions that emulate the different PA stages used to achieve a certain uplink transmit power level. The low- and high-power regions of the curve are separated by a device-specific threshold, $\gamma_{threshold}$. In principle, it is possible to empirically derive α and β parameters for different user equipment model versions.

To further simplify, the model defines idle, low, high and max power states which vary depending on the region of the curve the transmit power lies on. Since power consumption data for NR modems isn't publicly available yet, we assume a 10% increase for Low and High Power States for the measurements of a LTE modem operating at 2 GHz from the study in [5]. This assumption intends to account for the extra power consumption due to the different components and technologies, e.g. beamforming in the mmWave band, for NR. The UE power consumption due to uplink per transmit carrier is given by Eq. 5.2 and it is illustrated in Fig. 5.6. The parameters for the UE power consumption due to the UL can be found in Table 5.4. These parameters were derived in [5] in a controlled

Table 5.4: Parameters for UE Power Consumption due to Uplink [5]

RAT	LTE(2 GHz)	NR(28 & 26 GHz)
$\overline{P}_0$ (Micro Sleep)[mW]	25	25
$\overline{P}_1$ (Idle)[mW]	97	97
$\overline{P}_2$ (Low)[mW]	860	946
$\overline{P}_3$ (High)[mW]	1578	1736
$\overline{P}_4$ (Max)[mW]	2450	2450
$P_{c,max}$[W]	0.25	0.125
$\gamma_{threshold}$[dBm]	10	10

measurement setup without other power consuming components, e.g. the display.

$$P_{UE}(P_{tx}) = \begin{cases} \alpha_L \cdot P_{tx} + \beta_L & P_{tx} \leq \gamma \\ \alpha_H \cdot P_{tx} + \beta_H & P_{tx} > \gamma \end{cases} \tag{5.2}$$

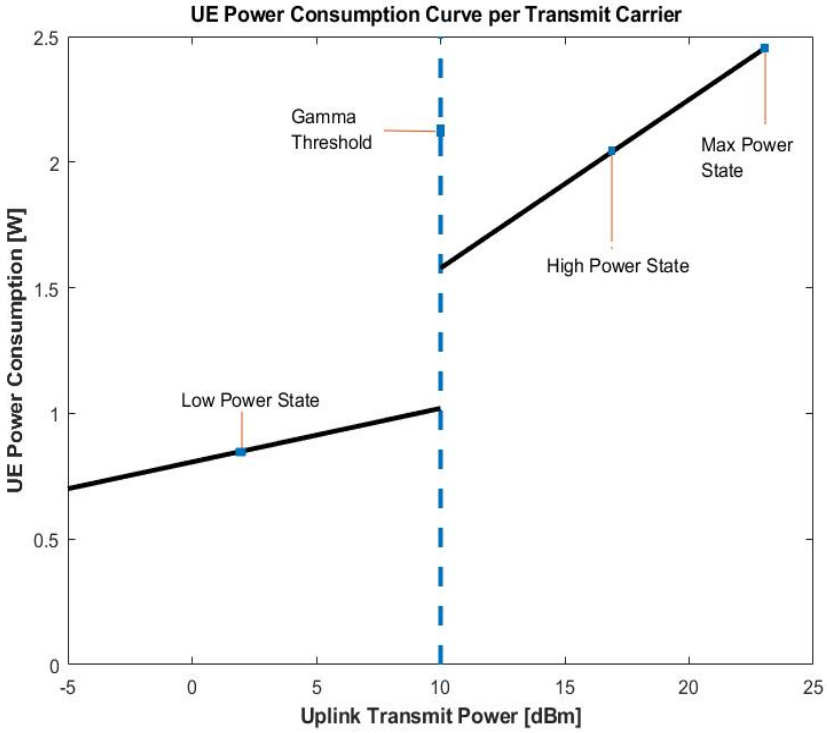

Figure 5.6: UE Power Consumption due to UL per Transmit Carrier adapted from [5]

Assumptions:

- Throughout this study we assume the UE uses multi-TX operation for multi-connectivity.

This means the UE can transmit on multiple radio access technologies at the same time limited by the maximum transmit power per carrier $P_{c,max}$, and also limited by the maximum transmit power across all carriers P_T (further detailed in Section5.6).

- We assume the PAs inside the modem are independent and thus the UE power consumption is summed when using carrier aggregation and/or multi-connectivity.

Given the assumptions, Eq. 5.3 describes the mathematical model for the UE power consumption due to UL.

$$P_{UL} = \sum_{BTS_i \subseteq AS}^{N_{conn}} N_{c,i} \cdot \overline{P}_{\{2,3,4\},i} \tag{5.3}$$

The P_{UL} term is dependent on the uplink transmit power for each carrier. The uplink transmit power dictates the power state of the user equipment $\overline{P}_{\{2,3,4\},i}$ for each connection. The power state for each connection is dependent on the transmit power given by the uplink power control mechanism. The uplink transmit power in turn is dependent on the pathgain experienced per connection. Each connection experiences a different pathgain which may vary as explained in Section 5.2. For instance, a UE employing LTE/NR DC (NR operating in the mmWave band) will experience different radio characteristics for each connection, e.g. the LTE modem on High Power State and the NR modem on Low Power State, and thus the user equipment may be on different power states simultaneously depending on the pathgain experienced on each connection.

The power states are mapped to the power level of each transmit carrier, thus the power state is multiplied by the number of carriers per connection $N_{c,i}$. The power consumption is summed for all the connections N_{conn}, i.e. for the active set of base stations providing services to a particular user.

5.3.2 UE POWER CONSUMPTION DUE TO THE DL

In downlink, the power consumption is mainly due to the DL data rate, i.e. the number of allocated resource blocks and baseband processing. Moreover, the power consumption is also dependent on the number of active carriers that determine the number of additional RF chains that need to be powered. The study in [5] specifies guidelines on how to extend the UE power consumption model to downlink for the device under-test used in our work. Eq. 5.4 describes the mathematical model for the UE power consumption due to DL employed in our study.

$$P_{DL} = N_{conn} \cdot N_c \cdot (\mu \cdot M + \delta) \tag{5.4}$$

The P_{DL} term is dependent on the number of resource blocks M, the number of carriers per connection N_c , and the number of base stations the user is simultaneously connected to N_{conn}. The μ term accounts for the power consumption per resource block and δ accounts for the power consumption due to the activation of an additional RF chain. The parameter values can be found on Table 5.5.

Assumptions:

- Each additional radio access technology requires the powering of an additional RF chain.
- The transmission of ACKs, baseband processing and decoding effort are taken into account with the given values for power consumption due to DL.

Table 5.5: Parameters for UE Power Consumption due to Downlink

Parameter	Value
μ [mW/RB]	0.8
δ [mW/ active carrier]	323

5.4 TRAFFIC MODEL

In our scenario we used a fixed packet size FTP Traffic model with an exponentially distributed inter-arrival time. The traffic model is designed in such a way that the number of offered bits is independent of the user throughput. Therefore, the amount of offered bits are the same for a different number of connections. The parameters are given in Table 5.6. In addition, we also employ the same traffic characteristics for both downlink and uplink traffic. The latter tries to address the fact that some use cases, e.g. social networking, are displaying symmetric traffic between uplink and downlink.

Table 5.6: Traffic Model Parameters

Parameter	Value
Session Distribution Time	Exponential
Mean Inter-arrival Time	1 s
Packet Size	5 MB
DL/UL ratio	1

5.5 MULTI-CONNECTIVITY FRAMEWORK

The study in [50] defines a multi-connectivity scheme labeled as BEST SINR, among others. This scheme is based on adding target secondary cells to users if the experienced DL SINR is above a predefined threshold. This threshold is dependent on the DL SINR from the master cell. Similarly, a disconnection threshold is used to disconnect secondary cells. This scheme will be used as a baseline scheme to show the multi-connectivity gains compared to single-connectivity. In addition, this work also details the mobility mechanisms for handover execution and the event of radio link failures which are relevant for our study. The handovers are executed if the DL SINR from the connected cell falls below the DL SINR from an adjacent cell. The reader can refer to the study in [46] for more details.

5.6 UPLINK POWER CONTROL FOR MULTI-CONNECTIVITY

In this study, we define the baseline uplink power control for multi-connectivity as shown in 1. The uplink power control mechanism implemented in our work is open-loop with fractional path loss compensation, as shown in Eq. 2.1. Following the recommendations given on the NR specification [4], we decided to first allocate the available transmit power of the user equipment to the LTE carries and subsequently allocate it to the NR carriers. The latter is to improve the robustness of the communication by allocating the necessary power to low-frequency link(s) first and then use the remaining power for the high-frequency links.

Algorithm 1 Fractional Path Loss Compensation for Multi-connectivity and Baseline Power Sharing for each UE

Input: $Available\ P_T, isDL, isUL, PL$

Output: $P_{PUSCH},\ Remaining\ P_T$

Initialization:

1: **for** $LTE\ Carriers$ **do**
2: $From\ Available\ P_T$:
3: $P_{PUSCH} = Power\ Control$
4: **end for**
5: **for** $NR\ Carriers$ **do**
6: $From\ Remaining\ P_T$:
7: $P_{PUSCH} = Power\ Control$
8: **end for**
9: **return** $P_{PUSCH}\ Remaining\ P_T$

Table 5.7: Uplink Power Control Parameters

Uplink Power Control	
Type	Fractional
α	0.8
M	55
P_T[W]	2.5
P_0[dBm]	-112

This uplink power control scheme intends to provide a realistic multi-connctivity extension of the state-of-the-art uplink power control mechanism. Each UE shares its available

transmit power P_T first for low frequency links and then for higher frequency links. As a baseline, the available transmit power is enough for maximum transmit power per carrier on three connections, i.e. TC.

The P_{PUSCH} is the transmit power per carrier. M stands for the number of resource blocks, P_0 for the target received power across all resource blocks, α a network configurable parameter related to fractional path-loss compensation, and PL accounts for the pathgain. The parameters are given in Table 5.7.

5.7 MULTI-CONNECTIVITY SCHEME

In this subsection, we propose a multi-connectivity scheme labeled as "Low UE Power State" which intends to reduce the UE power consumption when the user is in ACTIVE mode. The main goal of this scheme is to only add secondary connections that produce an uplink transmit power which lies in the low power region of the UE power consumption curve presented in Section 5.3.1. In addition, this scheme also avoids interference by adding secondary connections that avoid intra-frequency multi-connectivity.

Algorithm 2 Interference Avoidance and Low UE Power State Scheme

Input: $\phi_{\,threshold},\ Pathgain_{\,\forall BS},\ candidate\ BSs_{\,\forall UE},\ AS_{\,\forall UE}$

Output: $new\ AS_{\,\forall UE}$

Initialization : $candidate\ BSs = \emptyset$

1: **if** $\min(Pathgain_{\,\forall BS}) <= \ \phi_{\,threshold}$ **then**
2: $\quad candidate\ BSs_{\,\forall UE} = \ \min(Pathgain_{\,\forall BS})$
3: $\quad$ **for** $ue\ \in UE$ **do**
4: $\quad\quad \{candidate\ BSs\} = \ \{RAT(candidate\ BSs)\} \setminus \{RAT(AS)\}$
5: $\quad$ **end for**
6: **end if**
7: $AS_{\,\forall UE} = \ candidate\ BSs_{\,\forall UE}$
8: **return** $new\ AS_{\,\forall UE}$

The main purpose of this scheme is to reduce the UE power consumption by adding secondary connections that produce an uplink transmit power that lies within the low

power region of the UE power consumption curve given in Section 5.3.1. This approach avoids increased uplink transmit power levels for secondary connections in the high power region of the curve. The $\phi_{\,threshold}$ was derived by evaluating the upper bound uplink transmit power and solving for the pathgain. To be sure to avoid the high power region of the UE power consumption curve and avoid a ping-pong effect, we added a 1 dB margin with $\gamma_{\,threshold}$. The value is given in Table 5.8. Moreover, with this scheme the I_{MC} term from Equations 4.4 and 4.5 is avoided completely by connecting to secondary base stations from different radio access technologies, and thus different frequencies.

Table 5.8: Low UE Power State Scheme Parameters

Parameter	Value
$\phi_{\,threshold}[dB]$	92

6 RESULTS

This section presents the simulation experiments and the results of our work. Section 6.1 describe the experimental setups used to address our research questions. Section 6.2 presents the results regarding UE performance and power consumption based on experimental setup A. Section 6.4 presents the reliability gains using multi-connectivity in the city scenario presented on this work and it compares these gains with a simpler system scenario based on experiment setup B.

6.1 EXPERIMENTS

In order to obtain statistically good results, simulations must be rerun several times with slightly modified random input variables. To achieve this, simulators employ a pseudo-random number generator. This random number generator is initialized with a seed. The seed is any number (it doesn't have to be random) that's given as an input to the random number generator and creates the same sequence of random values for that seed. A different seed is used for each run.

For our simulations we conducted two types of experiments as described below:

Setup A: In order to test UE performance in terms of downlink/uplink throughput, power consumption and energy efficiency, we gradually increased the load for each simulation. We increased the load from 10 users up to 50 users. As the load increases we decreased the number of seeds in order to reduce simulation time. Table 6.1 shows the simulation parameters for this setup. In addition, with this experimental setup we test the effect on the uplink transmit power for the secondary connection with the new multi-connectivity scheme proposed in this work. The experimental **Setup A.1** employs the "Low UE Power State" multi-connectivity scheme as shown in Table 6.2.

Setup B: In order to test UE performance in terms of reliability, we performed simulations for a fixed number of users and gradually increase user speed. As described in Section 4, reliability in terms of mobility is quantified by the RLF rate. The RLF rate is defined as the time the user spends on RLF state divided by the total simulation time. For this setup,

Table 6.1: Simulation Parameters for Setup A

Simulation Parameters for Performance Studies	
Number of Seeds	10
Simulation Time	30 s
Simulation Type	Varying Load
User Speed	5 km/h
Deployment Type	3-Tier UDN
Deployment Configuration	9LTE+61NR1+61NR2
Multi-connectivity Scheme	BEST SINR
Environment	Manhattan City
Mobility Model	Street Movement
Propagation Model	ITU-R M.2135 and METIS version

Table 6.2: Simulation Parameters for Setup A.1

Multi-connectivity Scheme	Low UE Power State

we gradually increase the user speed from 10 km/h to 125 km/h. Table 6.3 illustrates the number of simulations per speed point and simulation time. Since users would have generally good radio conditions on a deployment with many base stations, we only use a $61NR1$ deployment configuration for this setup to study reliability.

Table 6.3: Simulation Parameters for Setup B

Simulation Parameters for Reliability Studies (City Scenario)	
Number of Seeds	10
Simulation Time	10 s
Simulation Type	Varying Speed
Number of Users	30
Traffic Model	Full Buffer
Deployment Type	1-Tier UDN
Deployment Configuration	61NR1
Multi-connectivity Scheme	BEST SINR
Environment	Manhattan City
Mobility Model	Street Movement
Propagation Model	ITU-R M.2135 and METIS version

In addition, results attained with experimental setup B were compared to a scenario using the COST-HATA propagation model and a random mobility walk. The latter was devel-

oped in [46]. In this setup, users are created on a random location and then start movement on a random direction. When they reach the edge of the deployment they bounce an imaginary circle with a random angle. Table 6.4 details the setup for this scenario.

Table 6.4: Simulation Parameters for General Case

Simulation Parameters for Reliability Studies (General Scenario)	
Number of Seeds	10
Simulation Time	10 s
Simulation Type	Varying Speed
Number of Users	30
Traffic Model	Full Buffer
Deployment Type	1-Tier UDN
Deployment Configuration	61NR1
Environment	No Scattering Objects
Mobility Model	Users Bounce inside Imaginary Circle
Propagation Model	COST-HATA

6.2 UE PERFORMANCE AND POWER CONSUMPTION FOR SETUP A

As depicted in Fig. 6.1, DC exhibits an average DL throughput gain of approximately 44% compared to SC for low load (15 users). TC exhibits a gain of approximately 2% with respect to DC (46% compared to SC). At mid load (45 users), the DC gain reduces to 18%. With TC, the average DL throughput reduces to 8% less compared to DC. This is due to the fact that interference increases faster when using TC due to the increased number of connections. In addition, there's more chance for intra-frequency MC which essentially hampers performance in an ultra-dense network.

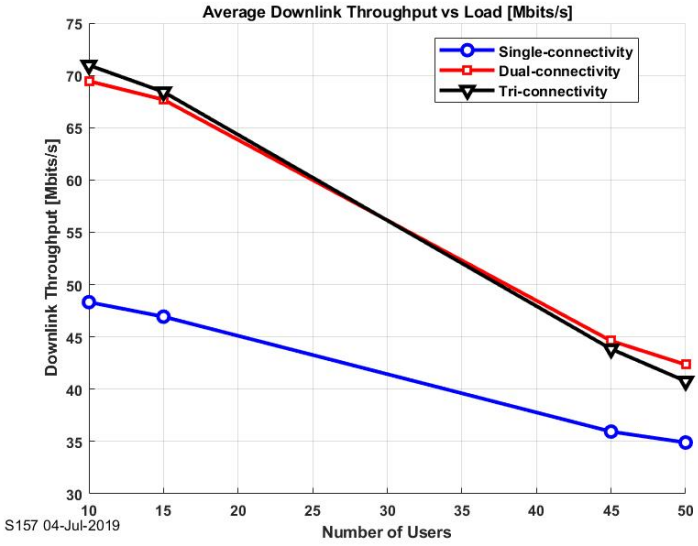

Figure 6.1: Average DL Throughput vs Load

With respect to the average uplink throughput at low loads, DC exhibits a gain of approximately 27% compared to SC, as shown in Fig. 6.2. The net performance in uplink is better than in downlink since the uplink interference is less in an ultra-dense network scenario at low load. TC exhibits a negative gain of approximately 2% compared to DC. The latter is due to the fact the BEST SINR MC scheme adds new secondary connections based exclusively on the DL SINR. Despite the increase in interference as the load increases, the uplink performance gain using DC compared to SC is kept and it only reduces to 18%. However, as shown in Fig. 6.2, interference decreases the uplink performance drastically. For even higher loads, the uplink and downlink performance with MC might become less

than with SC.

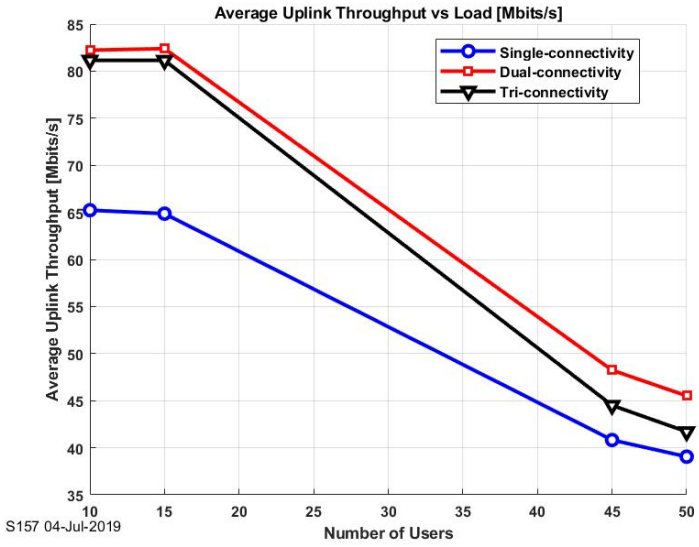

Figure 6.2: Average UL Throughput vs Load

In terms of UE power consumption, at low load, the increase compared to SC (853 mW) is 4% and 27% for DC (890 mW) and TC (1084 mW) respectively, as shown in Fig. 6.3a. However, as the load increases, the idle time of the UE decreases as well. Fig. 6.3b illustrates the fact that the UE power consumption is inversely correlated with the time the user spends in IDLE RRC state. As interference increases, the user spends more time in ACTIVE RRC state since the UE takes more time to transmit/receive data and thus the average UE power consumption increases. At mid load, the increase in average UE power consumption compared to SC (1139 mW) is 25% and 60% for DC (1427 mW) and TC (1825 mW) respectively.

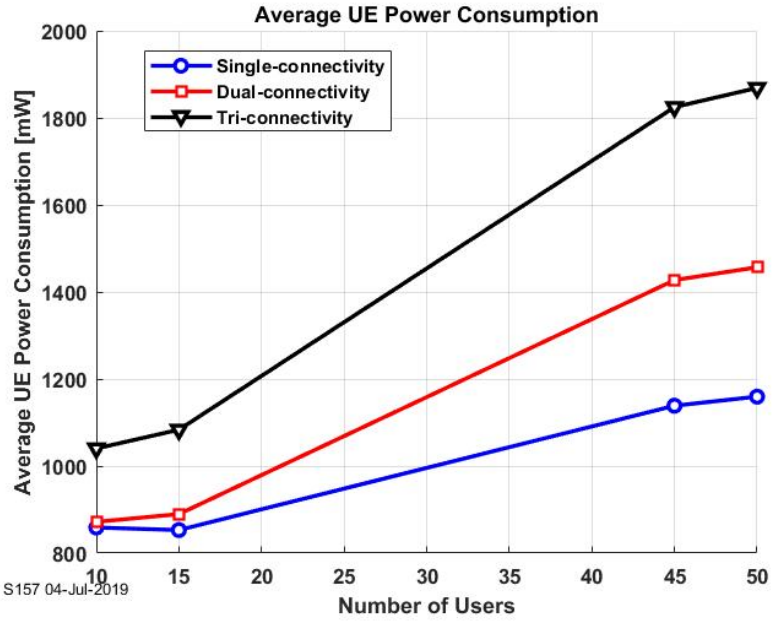

(a) Average UE Power Consumption [mW] vs Load

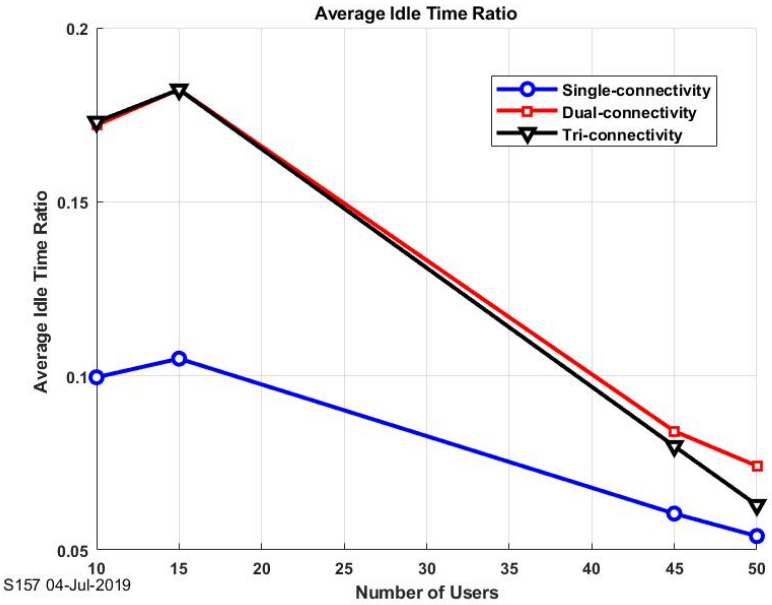

(b) Average Idle Time Ratio vs Load

Figure 6.3: Inverse Correlation between UE Power Consumption and Idle Time

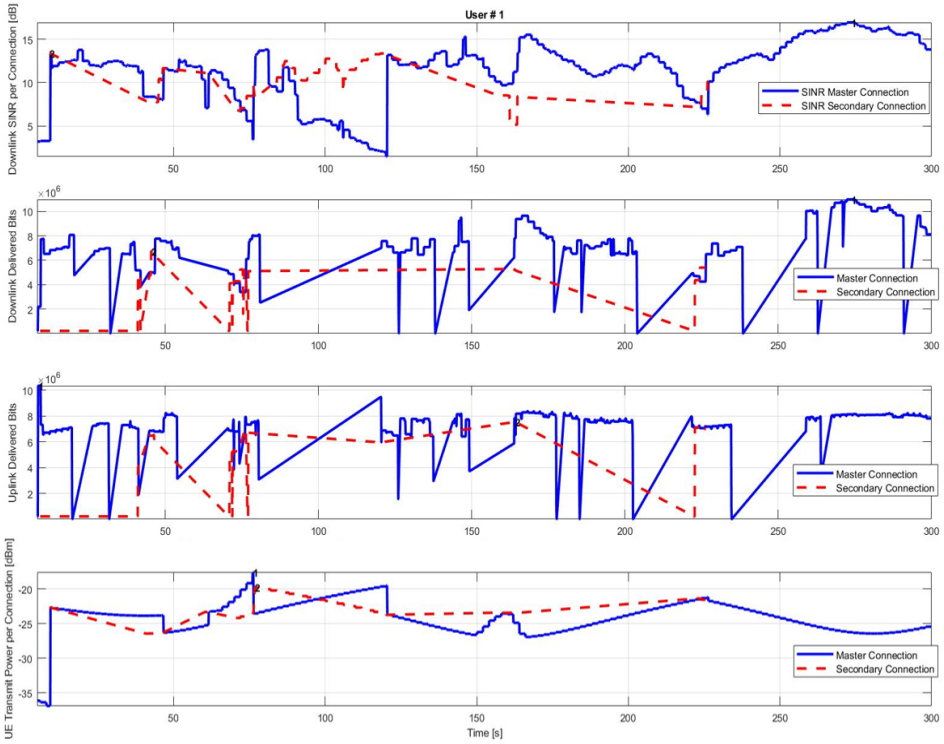

Figure 6.4: Time Plots for User 1 (loadpoint of 15 users): DL SINR per Connection, DL Delivered Bits, UL Delivered Bits, UE Transmit Power per Connection employing DC

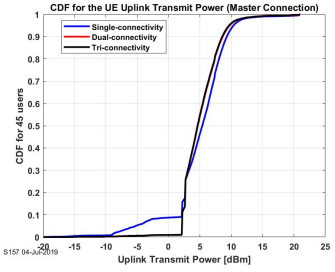

Figure 6.5: CDF for the UE Uplink Transmit Power (Master Connection)

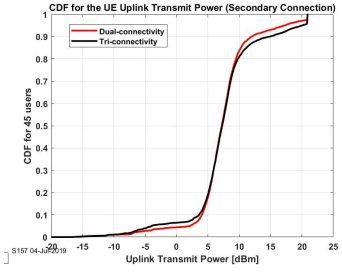

Figure 6.6: CDF for the UE Uplink Transmit Power (Secondary Connection)

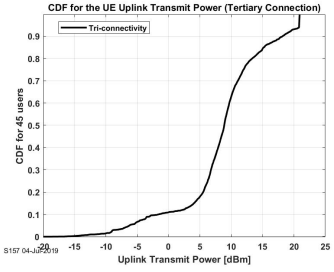

Figure 6.7: CDF for the UE Uplink Transmit Power (Tertiary Connection)

To illustrate the typical behavior of a user during the system-level simulations, the time plots in Figure 6.4 show the DL SINR, delivered bits in downlink and uplink, and the uplink transmit power per connection throughout the simulation. Figures 6.5, 6.6 and 6.7 illustrate the distribution of the uplink transmit power for the master, secondary and tertiary connection for different connection setups (SC, DC, TC). For instance, the transmit power for the master connection increases when the user employs multi-connectivity

as shown in Fig. 6.5. In addition, the transmit power for the master connection using multi-connectivity is seldom below 0 dBm. Moreover, the uplink transmit power for the secondary connection is less using DC than with TC for transmit powers above 10 dBm as shown in Fig. 6.6. By comparing Fig. 6.7 with Fig. 6.5 and 6.6 we can observe that the transmit power for the tertiary connection is higher than the transmit power for the master and secondary connection. The UE power consumption can be further reduced by reducing transmit power of the secondary connections with an appropriate multi-connectivity scheme.

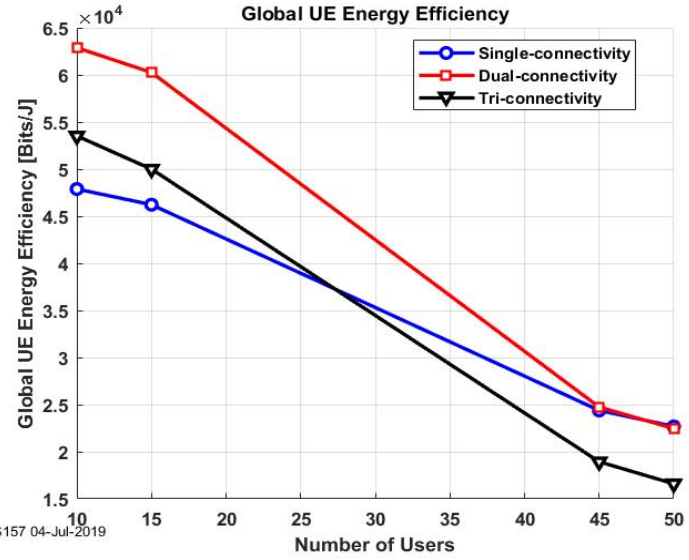

Figure 6.8: Average UE Energy Efficiency vs Load [Bits/J]

In terms of global UE energy efficiency, Fig. 6.8 shows that DC is the most energy efficient configuration for the user equipment. With this setup, DC displays a global UE energy efficiency of approximately 60 Kbits/J (approximately 30% more energy efficient than SC) at low loads. As shown in Fig. 6.3a, the margin between the average UE power consumption using DC and SC increases with load, however, the margin is small (at 4%) at low loads. At low loads, the improvement in UE performance employing DC causes the average UE power consumption to be comparable to that of SC since idle time is increased. The latter translates into superior global UE energy efficiency using DC. Energy efficiency reduces as the load increases and its gains disappear at mid load.

As shown in Fig. 6.9, the average DL UE energy efficiency is better even for TC at low loads than SC. Both, the average DL and UL UE energy efficiency is higher using

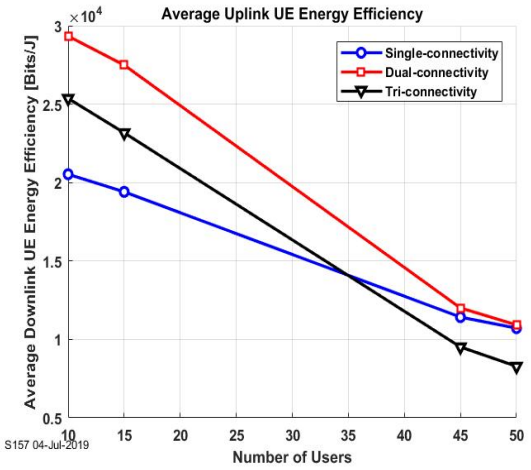

Figure 6.9: Average Downlink UE Energy Efficiency [Bits/J]

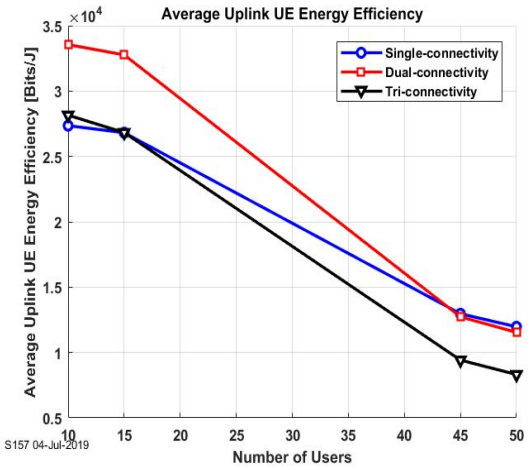

Figure 6.10: Average Uplink UE Energy Efficiency [Bits/J]

DC until the load increases up to 45 users as shown in Fig. 6.9 and 6.10. Using TC to transmit information is costly in terms of UL UE energy efficiency as it presents the worst performance as the load increases.

Another benefit of the use of multi-connectivity is the reduction of the RLF rate as the load increases. As shown in Fig. 6.11, multi-connectivity decreases the RLF rate at mid-load (45 users) by approximately 33% and 29% for DC and TC respectively. This behavior can be explained by the fact that the handover mechanism is based on the DL SINR. On an ultra-dense network the interference in downlink is high due to the increased number of base stations and the increased amount of reference signals sent in downlink. The results in Fig. 6.11 portray the fact that the usage of multi-connectivity within an ultra-dense network improve reliability by compensating for the poor DL SINR experienced when the load increases by having extra connections and thus avoid radio link failure. With multi-connectivity, the user needs to have poor radio conditions on all of its connected cells to enter into RLF state. The benefit of having secondary connections surpasses the additional interference multi-connectivity injects into the system.

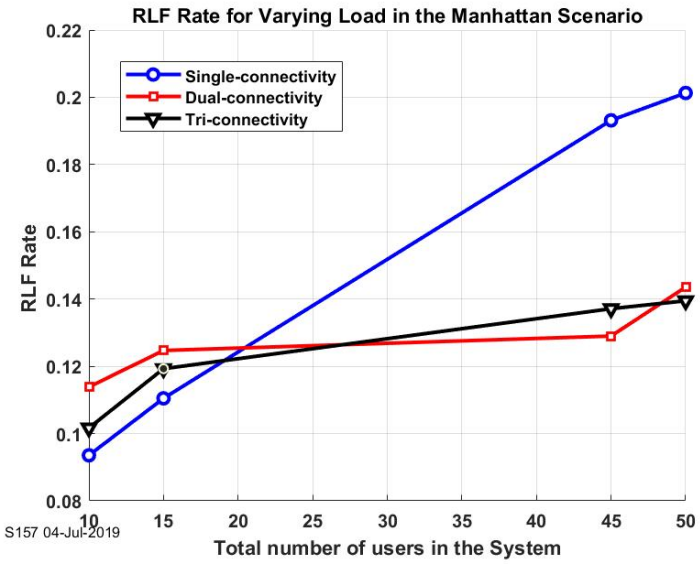

Figure 6.11: RLF Rate for Varying Load in the Manhattan Scenario

6.3 UPLINK TRANSMIT POWER REDUCTION FOR SETUP A.1

In this section we present the reduction of the uplink transmit power using the multi-connectivity scheme "Low UE Power State" proposed in our work. The Fig. 6.12 shows the CDF of the uplink transmit power for the secondary connection. With the Low UE Power State scheme, all UEs have an uplink transmit power less than 10 dBm for its secondary connection. Thus, the UEs remain in the low power state for the secondary connection and power consumption can be saved. In addition, with the Low UE Power State multi-connectivity scheme the secondary connections always employ a different radio access technology than its master connection and thus avoid intra-frequency multi-connectivity. Since connections to the master cell are based exclusively on the DL SINR, the master cell disregards the uplink transmit power level of the primary connection and thus the UE can still operate on the high power region of the power consumption curve. As shown in the Fig. 6.12, when the users employ the BEST SINR multi-connectivity scheme, an uplink transmit power of 10 dBm corresponds to the 80^{th} percentile. As shown in Fig. 6.12 the users above the 80^{th} percentile operate on the high power region of the UE power consumption curve.

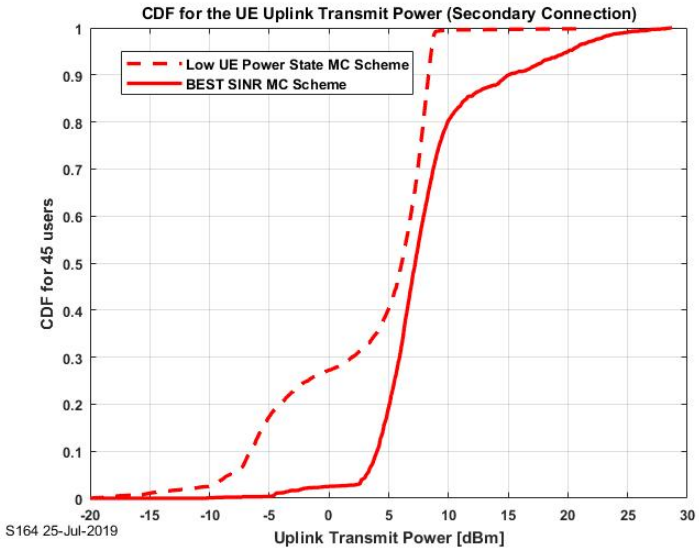

Figure 6.12: CDF for the Uplink Transmit Power of the Secondary Connection

These results show that the uplink transmit power can be reduced in an ultra-dense network. With this deployment, users are close to the antennas and thus the uplink transmit power can be maintained at a certain low level with the Low UE Power State multi-connectivity scheme.

6.4 RELIABILITY FOR SETUP B

This section conveys the multi-connectivity gains in terms of reliability for the city scenario and a general scenario based on the experimental Setup B. Reliability is studied in terms of mobility.

First, we display the gains of using multi-connectivity with varying speeds in terms of radio link failure with the city scenario presented in our work. Thereafter, for comparison purposes, we also display the reduction of RLF using multi-connectivity with a COST-HATA propagation model in conjunction with a generic mobility model. This generic mobility model is based on users bouncing inside an imaginary circle that encloses the network deployment.

Figure 6.13 illustrates the RLF rate behavior using multi-connectivity for varying speeds

in the urban city scenario based in experimental Setup B. As expected, the RLF rate increases as the user speed increases. The RLF rate evolves linearly . DC decreases RLF rate by approximately 20% compared to SC. TC doesn't show any relevant improvement in reducing RLF rate for our scenario. One possible explanation for this behavior might be the fact that small cells deployed in the streets always provide decent coverage to streets on LoS as depicted in Figure 5.2b. Since the users always move within the same street after their creation, the results might differ for a more comprehensive mobility model in which users turn on intersections.

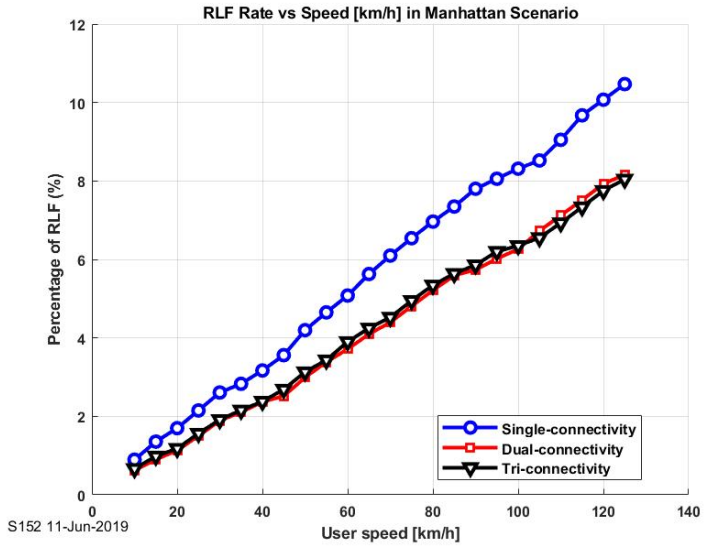

Figure 6.13: RLF Rate using Multi-connectivity for the Manhattan City Scenario

Figure 6.14 illustrates the RLF rate behavior using multi-connectivity for the general scenario based on the experimental Setup B. DC decreases the RLF rate by approximately 35% at high speeds compared to SC. In this scenario, TC does reduce the RLF rate even more. TC decreases the RLF rate by approximately 37% at high speeds compared to SC. The absence of the "street effect" of the Manhattan scenario could be one explanation for the additional reduction of the RLF rate when using TC in this scenario.

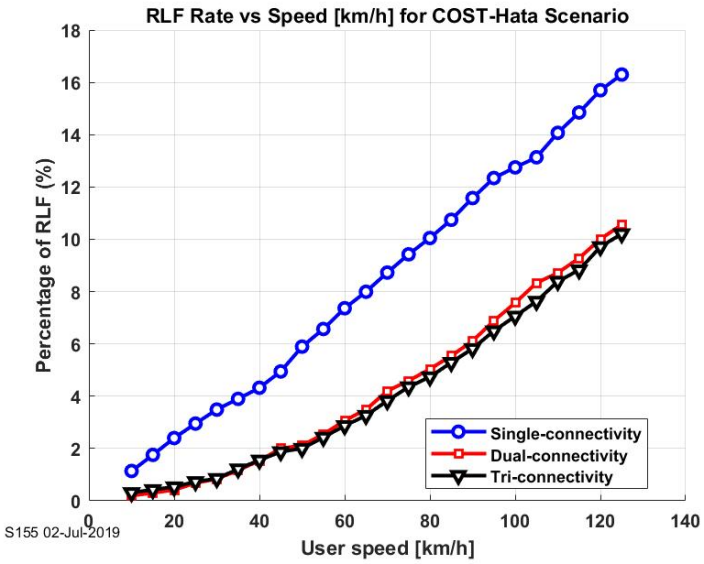

Figure 6.14: RLF Rate using Multi-connectivity for the COST-HATA Scenario

7 CONCLUSIONS

Our study focuses on the user equipment using multi-connectivity in an urban city scenario. This section discusses the findings related to our research questions. The impact of multi-connectivity on the UE performance is investigated in terms of user throughput, power consumption, energy efficiency and reliability.

In this study, we present a realistic urban city scenario that captures the propagation characteristics for the FR1 and FR2 bands. We extend a context-aware UE power consumption model mainly dependent on the user's uplink transmit power per connection. In addition, an uplink power control scheme for multi-connectivity to share the available transmit power of the user equipment for uplink transmissions is presented. Moreover, we demonstrate a multi-connectivity scheme to reduce uplink transmit power and avoid intra-frequency multi-connectivity. We perform simulations to study the performance of the user equipment.

Multi-connectivity increases downlink and uplink throughput for outdoor users in an urban city scenario. Gains in UE performance, with two and three connections, are achieved within a 3-tier ultra-dense network. For downlink, the gains using two connections compared to one are higher than using three connections compared to two. For uplink, the net performance in terms of user throughput is better than in downlink. However, TC exhibits less throughput than DC with the BEST SINR MC scheme since the latter disregards the uplink radio characteristics by adding secondary connections based exclusively on the DL SINR. Thus, DC is the best solution in terms of downlink and uplink throughput for our scenario.

The improved performance with multi-connectivity also increases the power consumption of the user equipment due to the use of extra RF chains and PAs. As the load increases, multi-connectivity causes a non trivial increase in the power consumption of the user equipment. The use of three connections induces a 60% increase in the average UE power consumption compared to one connection at mid load. The use of three connections is costly for the battery life but it still improves the RLF rate and user throughput.

In terms of energy efficiency, i.e. bits per Joule, the user equipment is more energy ef-

ficient using two connections provided there's a sufficient increase in performance with the secondary connection. At low load in downlink, it is more energy efficient for the user equipment to have multiple connections rather than one connection. For the same load in uplink, two connections is the most energy efficient configuration. In addition, within an ultra-dense network, the uplink transmit power for the secondary connection can be reduced by associating to those cells that produce an uplink transmit power below a certain threshold mapped with the low power operation of the PA of the user equipment. The latter is achieved with the Low UE Power State MC scheme.

Multi-connectivity produces a 20% decrease in the RLF rate at high speeds in urban city environments. Within an ultra-dense network, multi-connectivity still increases reliability in terms of mobility despite its challenges to provide radio coverage when NR is operating in the FR2 band. The latter means that fast-moving means of transportation can benefit from the use of multi-connectivity in urban city environments. However, there's an increasing need for more realistic user mobility models to know the full extent of these reliability gains.

8 DISCUSSION AND FUTURE WORK

This section discusses paths for future work and other scenarios that could be addressed to further reinforce our findings.

Throughout our work, we study UE performance for outdoor users in an urban city environment. However, presently, most mobile traffic is generated indoors. A study of UE performance and power consumption for indoor users would prove important in this regard since the indoor penetration loss is high for mmWave frequencies.

In our study, we employ a mobility model based on a simple street movement mobility model. There's a need for more comprehensive and random user mobility models for urban city scenarios. The performance of the user equipment employing multi-connectivity might change with more realistic mobility models for city scenarios, e.g. users moving in and out of buildings in a systematic manner or users turning on intersections.

Ultra-dense networks provide plenty of flexibility to design multi-connectivity schemes to tackle a certain metric. UE performance could be further improved by designing multi-connectivity schemes that decouple uplink and downlink cell association.

In addition, in our study, we employ an hexagonal deployment, i.e. a deterministic deployment. In real networks, the operators must decide on many factors in order to decide where to place their sites. Thus, a study that employs both a random deployment and stochastic geometry to model the different sizes of the coverage cells would prove useful in an urban city scenario.

Finally, the parameters for the UE power consumption model are specific for the device-under-test used in [5]. Further studies need to be done with empirically-driven parameters for different user equipment model versions in order to obtain fully generalizable results. The latter becomes more important given the heterogeneity of the modern user equipment.

9 SUSTAINABILITY

This section concerns the sustainability impacts of our study in the context of 5G, the user equipment, multi-connectivity, ultra-dense networks, and also urban city environments.

Currently, the radio access network is the main energy consumer in the mobile network [51]. However, in the future, with the advent of having an increasing number of mobile subscriptions and the advent of Internet of Things, the number of connected devices is increasing. The number of connected devices is expected to grow to 100 billion by 2030 [52]. The energy consumption of all these new devices might contribute in the same order of magnitude as the radio access network [53]. Thus, energy savings in the user equipment have a lot of potential from a macro perspective.

The power consumption of the user equipment using multi-connectivity increases in loaded scenarios, which is a common traffic scenario for urban environments. Although, as seen previously, the increase in power consumption can be mitigated by decreasing the uplink transmit power levels of the secondary connection with an appropriate multi-connectivity scheme in an ultra-dense network. Moreover, provided with enough additional increased performance, multi-connectivity generally improves the energy efficiency of the user equipment. It could also be possible to decrease the power consumption of the user equipment by compensating the extra instantaneous power consumption due to multi-connectivity by producing enough extra idle time.

Network densification in urban city environments means two things: First, multi-connectivity is most likely to increase the power consumption in the user equipment due to the increased loads and increased interference. Second, in order to tap into the benefits of multi-connectivity, network densification is required and the latter means the mobile network will consume more energy. Thus, in loaded urban city scenarios, multi-connectivity inexorably increases the power consumption on the user equipment but it is possible to reduce this increase while keeping acceptable QoS. Nevertheless, these solutions aim to improve the cost efficiency, energy efficiency and spectrum efficiency of providing capacity for services beyond 2020, thus making it a green solution given the IMT requirements.

Certainly, 5G will enhance other application fields and will enable novel applications and

services, e.g. the reduction of the RLF rate using multi-connectivity in urban city environments is an enabler for seamless mobility. And, these novel applications, in turn, could produce a CO_2 abatement in other sectors and also produce societal changes that could be more sustainable. 5G will serve as a catalyst for the Networked Society. We can further expand the sustainability impact of our study by encompassing social, individual, technical, environmental and economic aspects defined in [54]. The sustainability analysis including these aspects and its orders of effect is included in the Appendix section.

APPENDIX 1. ITU-R M.2135 Propagation Model from METIS-I

In this section, we provide additional details on the propagation model ITU-R M.2135 used in our work which was developed in METIS-I. As explained in Section 5, this model was modified for the FR2 band in order to match the field measurements done during the METIS project. In this section, we present the equations for the path loss model for urban environments at the FR1 band and the FR2 band for the macro and micro layer respectively.

Urban Macro for the FR1 Band

For LoS communication with a LTE macro base station operating in the FR1 band (UMa), the path loss is given by the Eq. A.1:

$$PL = 22.0log_{10}(d) \ + \ 28.0 \ + \ 20log_{10}(f_c) \quad 10m < d < D_{BP}$$

$$\begin{aligned} &PL = 40.0log_{10}(d_1) \ + \ 7.8 \ - \ 18.0log_{10}(h_{BS}) - \ 18.0log_{10}(h_{UE}) \ + \ 2.0log_{10}(f_c) \\ &d_{BP} < d < 5000m \ with \ h'_{UE} = 1m \end{aligned} \tag{A.1}$$

For nLoS communication with a LTE macro base station (UMa) where the base station is located on rooftops, most of the signal reaches users through diffraction. The path loss is given by the Eq. A.2:

$$PL = \begin{cases} L_{fs} + L_{rts} + L_{msd} \, if \ L_{rts} + L_{msd} > 0 \\ L_{fs} \qquad\qquad\qquad\qquad if \ L_{rts} + L_{msd} \leq 0 \end{cases} \tag{A.2}$$

The total path loss is the sum of the free space loss L_{fs}, the diffraction loss from the rooftops to the street L_{rts} and a reduction due to multiple screen diffraction past rows of buildings L_{msd}. The reader can refer to the METIS technical deliverable D.61 [25] for more details on the computation of these diffraction terms.

Urban Micro for the FR2 Band

For LoS communication with an NR micro base station operating in the FR2 band (UMi), the path loss is given by the Eq. A.3:

$$PL = 22.0log_{10}(d) + 28.0 + 20log_{10}(f_c) + PL_{offset} \quad 10m < d < D_{BP}$$

$$\begin{aligned} &PL = 40.0log_{10}(d_1) + 7.8 - 18.0log_{10}(h'_{BS}) - 18.0log_{10}(h'_{UE}) + 2.0log_{10}(f_c) + \\ &PL_{offset}\ for\ d_{BP} < d < 5000\ m\ with\ h'_{UE} = 1m \end{aligned} \tag{A.3}$$

Note that this propagation model is adapted with the PL_{offset} to match the FR2 band's field measurements done during the METIS project.

For nLoS communication with an NR micro base station, i.e. connectivity with users in perpendicular streets with respect to the base stations, operating in the FR2 band (UMi), the path loss is given by the Eq. A.4:

$$\begin{aligned} &PL = min(PL(d_1, d_2), PL(d_2, d_1)) \\ &PL(d_k, d_l) = PL_{LoS}(d_k) + 17.9 - 12.5n_j + 10n_jlog_{10}(d_l) + 3log_{10}(f_c) \\ &n_j = max(2.8 - 0.0024d_k, 1.84) \\ &PL_{LoS} : path\ loss\ of\ scenario\ UMi\ LoS\ and\ k, l\ in\ 1, 2. \end{aligned} \tag{A.4}$$

d_1 and d_2 are defined with respect to the Manhattan grid. d_1 is the distance from the base station to the center of the next perpendicular street along its LoS path. d_2 is the distance where the UE is located along the perpendicular street measured from the center of the LoS street.

For Outdoor-to-Indoor (O2I) communication in both the FR1 and FR2 band, the path loss

is given by Eq. A.5:

$$
\begin{aligned}
PL &= PL_{out} + PL_{tw} + PL_{in} \\
PL_{out} &= PL(d_{out} + d_{in}) \\
PL_{tw} &= 9.82 + 5.98 log_{10}(f_c) \; + \; 15 \cdot (1 \; - \; sin(\theta))^2 \\
PL_{in} &= 0.5 d_{in}
\end{aligned}
\tag{A.5}
$$

Moreover, the Minimum Coupling Loss (MCL) is defined in order to have a minimum path loss when the users are close to the base stations as shown in Eq. A.6.

$$
PL = min(MCL, PL) \tag{A.6}
$$

APPENDIX 2. Sustainability Analysis

In this section, we present a sustainability analysis defined in [6] to analyze the sustainability impact of our work.

Figure 9.1: Sustainability Analysis based on the guidelines defined in [6]

References

[1] A.-l. Kor, E. Rondeau, K. Andersson, J. Porras, A.-l. Kor, E. Rondeau, K. Andersson, J. Porras, and J.-p. G. Education, "Education in green ICT and control of smart systems : A first hand experience from the International PERCCOM masters programme," *12th FAC Symposium on Advances in Control Education*, 2019.

[2] Ericsson, "Ericsson Mobility Report_June_2019," *White Paper*, no. June, 2019. [Online]. Available: https://www.ericsson.com/49d1d9/assets/local/mobility-report/documents/2019/ericsson-mobility-report-june-2019.pdf

[3] T. Specification, G. Radio, A. Network, N. Generation, and A. Technologies, "3gpp tr 38.913," vol. 0, no. Release 15, 2018.

[4] S. P. E. Dahlman and J. Sköld, "5G NR: The Next Generation Wireless Access Technology," *Academic Press*, 2018.

[5] R. Falkenberg, B. Sliwa, and C. Wietfeld, "Rushing Full Speed with LTE-Advanced Is Economical - A Power Consumption Analysis," *IEEE Vehicular Technology Conference*, vol. 2017-June, 2017.

[6] C. Becker, S. Betz, R. Chitchyan, L. Duboc, S. M. Easterbrook, B. Penzenstadler, N. Seyff, and C. C. Venters, "Requirements: The key to sustainability," *IEEE Software*, vol. 33, no. 1, pp. 56–65, 2016.

[7] Ericsson, "Ericsson Mobility Report, June 2018," no. June, 2018. [Online]. Available: https://www.ericsson.com/491e17/assets/local/mobility-report/documents/2018/ericsson-mobility-report-june-2018.pdf

[8] ——, "Mobility Report," *White Paper*, no. May, 2016. [Online]. Available: https://www.ericsson.com/res/docs/2016/ericsson-mobility-report-2016.pdf

[9] A. Osseiran, F. Boccardi, V. Braun, K. Kusume, P. Marsch, M. Maternia, O. Queseth, M. Schellmann, H. Schotten, H. Taok, H. Tullberg, M. A. Uusitalo, B. Timus, M. Fallgren, and Afif, "Scenarios for 5G Mobile and Wireless Communications : The Vision of the METIS Project Scenarios for the 5G M obile and Wireless Communications :," no. January 2016, pp. 26–35, 2014.

[10] M. K. Tsai, "Cloud 2.0 clients and connectivity - Technology and challenges," *Digest of Technical Papers - IEEE International Solid-State Circuits Conference*, vol. 57, pp. 15–19, 2014.

[11] Y. Huo, X. Dong, and W. Xu, "5G cellular user equipment: From theory to practical hardware design," *IEEE Access*, vol. 5, pp. 13 992–14 010, 2017.

[12] T. Specification and G. Services, *3gpp tr 21.866*, 2017, vol. 0, no. Release 15.

[13] M. Lauridsen, G. Berardinelli, F. M. Tavares, F. Frederiksen, and P. Mogensen, "Sleep modes for enhanced battery life of 5G mobile terminals," *IEEE Vehicular Technology Conference*, vol. 2016-July, 2016.

[14] E. Mohyeldin, "Minimum Technical Performance Requirements for IMT-2020 radio interface (s) Eiman Mohyeldin ITU-R Workshop on IMT-2020 terrestrial radio interfaces," 2016.

[15] D. Final and D. Kennedy, "Euro-5G Supporting the European 5G Initiative D2.6 Final report on programme progress and KPIs," 2017. [Online]. Available: https://5g-ppp.eu/wp-content/uploads/2017/10/Euro-5G-D2.6_Final-report-on-programme-progress-and-KPIs.pdf

[16] H. Elshaer, F. Boccardi, M. Dohler, and R. Irmer, "Downlink and Uplink Decoupling: A disruptive architectural design for 5G networks," *2014 IEEE Global Communications Conference, GLOBECOM 2014*, pp. 1798–1803, 2014.

[17] F. B. Tesema and A. Awada, "Fast Cell Select for Mobility Robustness in Intra-frequency 5G Ultra Dense Networks," 2016.

[18] N. P. Kuruvatti, J. F. Molano, and H. D. Schotten, "Mobility context awareness to improve Quality of Experience in traffic dense cellular networks," *Proceedings of the 24th International Conference on Telecommunications: Intelligence in Every Form, ICT 2017*, 2017.

[19] F. B. Tesema, A. Awada, I. Viering, M. Simsek, and G. Fettweis, "Evaluation of Context-Aware Mobility Robustness Optimization and Multi-Connectivity in Intra-Frequency 5G Ultra Dense Networks," *IEEE Wireless Communications Letters*, vol. 5, no. 6, pp. 608–611, 2016.

[20] M. Kamel, S. Member, W. Hamouda, and S. Member, "Ultra-Dense Networks : A Survey," vol. 18, no. 4, pp. 2522–2545, 2019.

[21] Ö. Bulakci, M. Ericson, A. Prasad, E. Pateromichelakis, J. Belschner, P. Arnold, and G. Calochira, "RAN Enablers for 5G Radio Resource Management," pp. 1–6, 2017.

[22] A. Prasad, F. S. Moya, M. Ericson, R. Fantini, and Ö. Bulakci, "Enabling RAN moderation and dynamic traffic steering in 5G," *IEEE Vehicular Technology Conference*, 2017.

[23] J.-E. Berg, "A recursive method for street microcell path loss calculations," *Proceedings of 6th International Symposium on Personal, Indoor and Mobile Radio Communications*, vol. 1, pp. 3–6, 1995.

[24] A. Rauch, J. Lianghai, A. Klein, and H. D. Schotten, "Fast algorithm for radio propagation modeling in realistic 3-D urban environment," *Advances in Radio Science*, vol. 13, no. 2013, pp. 169–173, 2015.

[25] D. Number, P. Name, and T.-t. I. Society, "Deliverable D6 . 1 Simulation guidelines," 2013.

[26] Report ITU-R M.2135-1, "Guidelines for evaluation of radio interface technologies for IMTadvanced," *Evaluation*, vol. 93, no. 3, 2009. [Online]. Available: http://www.ncbi.nlm.nih.gov/pubmed/19923880

[27] A. T. E. Sites, "Combining 5G NR with LTE," pp. 1–12.

[28] V. Petrov, D. Solomitckii, A. Samuylov, M. A. Lema, M. Gapeyenko, D. Moltchanov, S. Andreev, V. Naumov, K. Samouylov, M. Dohler, and Y. Koucheryavy, "Dynamic Multi-Connectivity Performance in Ultra-Dense Urban mmWave Deployments," *IEEE Journal on Selected Areas in Communications*, vol. 35, no. 9, pp. 2038–2055, 2017.

[29] M. Lauridsen, P. Mogensen, and L. Noël, "Empirical LTE smartphone power model with DRX operation for system level simulations," *IEEE Vehicular Technology Conference*, no. 1, pp. 0–5, 2013.

[30] M. Lauridsen, "Studies on Mobile Terminal Energy Consumption for LTE and Future 5G," 2014. [Online]. Available: http://vbn.aau.dk/files/206141678/master_Lauridsen.pdf

[31] M. Lauridsen, P. Mogensen, and T. B. Sørensen, "Estimation of a 10 Gb/s 5G receiver's performance and power evolution towards 2030," *2015 IEEE 82nd Vehicular Technology Conference, VTC Fall 2015 - Proceedings*, 2016.

[32] I. L. Da Silva, G. Mildh, M. Saily, and S. Hailu, "A novel state model for 5G Radio Access Networks," *2016 IEEE International Conference on Communications Workshops, ICC 2016*, pp. 632–637, 2016.

[33] A. Simonsson and A. Furuskär, "Uplink power control in LTE - Overview and performance: Principles and benefits of utilizing rather than compensating for SINR variations," *IEEE Vehicular Technology Conference*, pp. 1–5, 2008.

[34] T. Specification, G. Radio, and A. Network, "3gpp ts 38.101-3," vol. 0, no. Release 15, 2018.

[35] M. Lauridsen, G. Berardinelli, T. B. Sørensen, and P. Mogensen, "Ensuring energy efficient 5G user equipment by technology evolution and reuse," *IEEE Vehicular Technology Conference*, vol. 2015-Janua, no. January, 2014.

[36] T. Tirronen, A. Larmo, J. Sachs, B. Lindoff, and N. Wiberg, "Reducing energy consumption of LTE devices for machine-to-machine communication," *2012 IEEE Globecom Workshops, GC Wkshps 2012*, pp. 1650–1656, 2012.

[37] M. S. Mushtaq, S. Fowler, and A. Mellouk, "Power saving model for mobile device and virtual base station in the 5G era," *IEEE International Conference on Communications*, pp. 1–6, 2017.

[38] E. For and O. Of, "An efficient method for Minimizing Energy Consumption of User Equipment in Storage-embedded Heterogeneous Networks," no. August, pp. 70–76, 2014.

[39] K. Zhang, Y. Mao, S. Leng, Q. Zhao, L. Li, X. Peng, L. Pan, S. Maharjan, and Y. Zhang, "Energy-Efficient Offloading for Mobile Edge Computing in 5G Heterogeneous Networks," *IEEE Access*, vol. 4, pp. 5896–5907, 2016.

[40] D. Temesgene, "Offloading for Mobile Device Performance Improvement Cyber foraging," pp. 7421–7430, 2019.

[41] P. Frenger and M. Ericson, "Assessment of alternatives for reducing energy consumption in multi-RAT scenarios," *IEEE Vehicular Technology Conference*, vol. 2015-Janua, no. January, pp. 2–6, 2014.

[42] F. Boccardi, J. Andrews, H. Elshaer, M. Dohler, S. Parkvall, P. Popovski, and S. Singh, "Why to decouple the uplink and downlink in cellular networks and how to do it," *IEEE Communications Magazine*, vol. 54, no. 3, pp. 110–117, 2016.

[43] D. Xenakis, N. Passas, L. Merakos, and C. Verikoukis, "Mobility management for femtocells in LTE-advanced: Key aspects and survey of handover decision algorithms," *IEEE Communications Surveys and Tutorials*, vol. 16, no. 1, pp. 64–91, 2014.

[44] D. Xenakis, N. Passas, and C. Verikoukis, "An energy-centric handover decision algorithm for the integrated LTE macrocell-femtocell network," *Computer Communications*, vol. 35, no. 14, pp. 1684–1694, aug 2012. [Online]. Available: https://www.sciencedirect.com/science/article/pii/S0140366412001491

[45] X. Shao, Z. Gao, W. Zhou, H. Liu, and Y. Wang, "A Multi-Criteria Handover Algorithm for UE Energy Efficiency and Cell Load Balance in Dense HetNets," *2016 19th International Symposium on Wireless Personal Multimedia Communications (WPMC)*, no. c, pp. 14–18, 201602.

[46] S. Engineering, "Valentin Poirot ENERGY EFFICIENT MULTI-CONNECTIVITY FOR ULTRA-DENSE," 2017.

[47] Li Chen, Wenwen Chen, Bin Wang, Xin Zhang, Hongyang Chen, and Dacheng Yang, "System-level simulation methodology and platform for mobile cellular systems," *IEEE Communications Magazine*, vol. 49, no. 7, pp. 148–155, 2011. [Online]. Available: http://ieeexplore.ieee.org/lpdocs/epic03/wrapper.htm?arnumber=5936168

[48] L. Raschkowski, P. Kyösti, K. Kusume, and T. Jamsa, "METIS D1.4: Summary METIS channel models," no. July, pp. 1–30, 2015.

[49] B. Dusza, P. Marwedel, O. Spinczyk, and C. Wietfeld, "A context-aware battery lifetime model for carrier aggregation enabled LTE-A systems," *2014 IEEE 11th Consumer Communications and Networking Conference, CCNC 2014*, pp. 13–19, 2014.

[50] V. Poirot, M. Ericson, M. Nordberg, and K. Andersson, "Energy efficient multi-connectivity algorithms for ultra-dense 5G networks," *Wireless Networks*, vol. 0123456789, 2019. [Online]. Available: https://doi.org/10.1007/s11276-019-02056-w

[51] M. Gruber, O. Blume, D. Ferling, D. Zeller, M. Imran, and E. Strinati, "EARTH - Energy Aware Radio and Network Technologies," *Personal, Indoor and Mobile Radio Communications, 2009 IEEE 20th International Symposium on*, pp. 1–5, 2009.

[52] Global e-Sustainability Initiative, "#SMARTer2030-ICT Solutions for 21st Century Challenges," pp. 1–8, 2015. [Online]. Available: http://smarter2030.gesi.org

[53] D. G. Connect, "5G and Energy Efficiency," no. November, 2017.

[54] J. P. L. Duboc, "Do we really know what we are building? Raising awareness of potential Sustainability Effects of Software Systems in Requirements Engineering," *International Requirements Engineering Conference*, 2019.